Theses and Dissertations--Psychology   Psychology

2024

Characterizing Resting Cerebral Blood Flow in Obsessive-Compulsive Disorder with Arterial Spin Labeling

Hannah R. Wild
University of Kentucky, hwild012@gmail.com
Author ORCID Identifier:
 https://orcid.org/0000-0002-0172-7565
Digital Object Identifier: https://doi.org/10.13023/etd.2024.148

Right click to open a feedback form in a new tab to let us know how this document benefits you.

CHARACTERIZING RESTING CEREBRAL BLOOD FLOW IN
OBSESSIVE-COMPULSIVE DISORDER WITH ARTERIAL SPIN LABELING

THESIS

A thesis submitted in partial fulfillment of the
requirements for the degree of Master of Science in the
College of Arts and Sciences
at the University of Kentucky

By
Hannah R. Wild
Director: Dr. Thomas Adams, Assistant Professor of Clinical Psychology
Lexington, KY
2024

ABSTRACT OF THESIS

CHARACTERIZING RESTING CEREBRAL BLOOD FLOW IN
OBSESSIVE-COMPULSIVE DISORDER WITH ARTERIAL SPIN LABELING

Obsessive-compulsive disorder (OCD) is a condition characterized by intrusive thoughts (obsessions) and ritualistic behaviors (compulsions) profoundly impacting daily functioning and quality of life. Neuroimaging studies using various techniques have revealed inconsistent resting cerebral blood flow (rCBF) patterns in OCD patients, particularly within the cortico-striatal-thalamo-cortical (CSTC) circuit and sensorimotor network. Arterial Spin Labeling (ASL) MRI offers a promising, noninvasive method for directly measuring rCBF. This study, using data from the Yale HCP Trio study, analyzed unmedicated OCD patients and healthy controls, who underwent two consecutive resting pulsed-ASL scans. OCD patients with lower obsessional severity exhibited higher perfusion in the pre- and postcentral gyri, indicating potential sensorimotor circuit dysregulation. However, no other results survived FDR correction. Interestingly, highly obsessional OCD patients did not show increased sensorimotor perfusion, relative to HCs, suggesting potential differences in cognitive processes during rest (e.g., obsessing, rather than mind-wandering). Future investigations should explore perfusion differences across OCD severity levels, considering individual differences in obsession type and cognitive processes at rest to better characterize group differences in rCBF.

KEYWORDS: obsessive-compulsive, arterial spin labeling, perfusion, resting-cerebral-blood flow

Hannah Wild
_____
Name of Student

3/31/2024
_____
Date

CHARACTERIZING RESTING CEREBRAL BLOOD FLOW IN
OBSESSIVE-COMPULSIVE DISORDER WITH ARTERIAL SPIN LABELING

By

Hannah Wild

<table>
<tr><td>Thomas Adams, Ph.D.</td></tr>
<tr><td>Director of Thesis</td></tr>
</table>

<table>
<tr><td>Michael Bardo, Ph.D.</td></tr>
<tr><td>Director of Graduate Studies</td></tr>
</table>

<table>
<tr><td>3/31/2024</td></tr>
<tr><td>Date</td></tr>
</table>

ACKNOWLEDGMENTS

TABLE OF CONTENTS

LIST OF TABLES

LIST OF FIGURES

CHAPTER 1. INTRODUCTION

1.1   Background

Obsessive-compulsive disorder (OCD) is characterized by pervasive and recurrent obsessions (i.e., intrusive or unwanted thoughts, urges, or images) or compulsions (i.e., repetitive, ritualistic mental or behavioral acts performed to reduce distress typically associated with an obsession) that cause significant distress, disrupt normal functioning, or consume more than an hour per day (American Psychiatric Association [APA], 2013; Foa et al., 1995). The twelve-month prevalence of OCD is approximately 1.2% (Kessler et al., 2005; Ruscio et al., 2010), although subclinical OCD symptoms are much more common, affecting up to 21-25% of people (Fullana et al., 2009). OCD may be chronic or episodic (Ravizza et al., 1997) and is associated with significant impairments in daily functioning and quality of life (Koran et al., 1996).

OCD is associated with widespread neural abnormalities. Dysfunction has been reported in multiple functional circuits, including, but not limited to, the cortico-striatal-thalamo-cortical (CSTC) circuit (Graybiel & Rauch, 2000) and canonical fear circuitry (Milad & Rauch, 2012). OCD is also associated with dysconnectivity within and between large-scale intrinsic networks such as the default mode network (DMN), salience network (SN), sensorimotor network, and central executive network (CEN; Gürsel et al., 2018), but the location, direction, and magnitude of abnormalities vary dramatically across studies. These inconsistencies may be attributed to differences in fMRI parameters used (e.g., types of masks, sequences, or analyses), sample composition (e.g., medication

status, demographics, and OCD subtype/severity), and study procedures (e.g., resting vs. task-based).

Research has reliably demonstrated abnormalities in the medial prefrontal cortex (mPFC) among OCD patients. Specific ROIs within the larger mPFC complex are major hubs in the CSTC circuit, fear circuit, CEN, DMN, and SN (Menon, 2011; Milad & Rauch, 2012). Symptom provocation paradigms suggest that, compared with healthy controls (HCs), OCD patients exhibit decreased ventral mPFC (vmPFC) activation in response to OCD-specific fear-inducing stimuli (Banca et al., 2015), but increased vmPFC activation in response to non-specific fear-inducing stimuli (An et al., 2009). Similarly, patterns of orbital frontal cortex (OFC) hyper- and hypoactivation in OCD likely differ between lateral (Rauch et al., 1994) and medial portions of the OFC (Milad & Rauch, 2007; Rauch et al., 2007). Specifically, compared to HCs, OCD patients have demonstrated lateral OFC (lOFC) hyperactivation and medial OFC (mOFC) hypoactivation during OCD symptom provocation (Milad & Rauch, 2007; Rauch et al., 1994). In addition, OCD patients have repeatedly demonstrated anterior cingulate cortex (ACC) hyperactivation, broadly, in response to OCD-related symptom provocation tasks (Adler et al., 2000; Breiter et al., 1996; McGuire et al., 1994; Rauch et al., 1994). Although ACC hyperactivity has been noted as a key abnormality underlying OCD pathophysiology (Saxena et al., 2009), the functional roles of ACC subregions are quite diverse, and patterns of task-based activation may highly depend on task characteristics (Bush et al., 2000; Etkin et al., 2011).

1.2   Resting Cerebral Blood Flow

Several neuroimaging methods are available to examine resting neuronal activation. For example, the amplitude of low-frequency fluctuations (ALFF) of blood oxygen level-dependent (BOLD) signal can be used to index region-specific, spontaneous neural activity (M. D. Fox & Raichle, 2007; Zang, et al., 2007; Zou et al., 2008). Multiple studies have examined regional abnormalities in ALFF associated with OCD, but results are inconsistent (Zhang et al., 2021; Bu et al., 2019; J. Fan et al., 2017; Hou et al., 2012; Li et al., 2011; J. Liu et al., 2021; Long et al., 2021; J.-D. Ma et al., 2021; Y. Ma et al., 2021; Xia et al., 2019, 2020; Zhao et al., 2017; Zhu et al., 2015, 2016; Yang et al., 2019). However, one consistent finding emerged from a recent mega-analysis, demonstrating decreased fractional ALFF in the bilateral sensorimotor cortex, the right parieto-occipital cortex, and bilateral postcentral gyri (Bruin et al., 2023), indicating OCD patients demonstrate hypoactivation in sensorimotor regions, relative to HCs.

Like other BOLD studies, inconsistencies in the ALFF literature could be attributed to between-study differences in individual paradigms or sample composition. Specifically, between studies there is substantial heterogeneity in OCD symptoms and sub-types (e.g., obsessions about contamination vs. symmetry), presence of comorbidities (e.g., anxiety, depression), and/or medication status (e.g., drug-naïve, drug-washout, or medicated; Beucke et al., 2013). For example, four studies of unmedicated OCD patients have reported increased ALFF in the mPFC; though specific ROIs varied dramatically across studies (Bu et al., 2019; J. Liu et al., 2021; Xia et al., 2019; Yang et al., 2019). Although some studies using mixed samples of medicated and unmedicated OCD patients have also reported increased ALFF in the mPFC (Hou et al., 2012; Zhu et al.,

2016), others have reported decreased ALFF in the mPFC, specifically, the left pregenual ACC (Long et al., 2021).

Inconsistencies in ALFF OCD literature may also, in part, be due to the use of BOLD as a functional localizer. BOLD signal comes primarily from intravascular deoxygenated hemoglobin (dHB). However, the actual activation site and dHB location are somewhat dissociated (Borogovac & Asllani, 2012; Hoogenraad et al., 2001). Regions isolated with BOLD may reflect spatial spreading into feeding arterial and draining venous structures, which are further removed from the tissue than more closely coupled venules and capillaries within the parenchyma (Borogovac et al., 2010). Above all, BOLD signal represents a composite of changing cerebral blood flow (CBF), cerebral blood volume, and oxygen consumption. As an aggregate signal, specific physiological correlates related to neuronal activity cannot be isolated (Borogovac et al., 2010). BOLD is, therefore, less directly interpretable as a precise correlate of neural metabolic activity. Also, the BOLD signal is commonly expressed as a percent change in activation (e.g., neural activation at baseline vs. task conditions), which generally shows where neural activity changes, but it does not offer quantifiable information regarding differences in baseline values of CBF (Shulman et al., 2007).

Positron emission tomography (PET), single-photon emission computerized tomography (SPECT), and arterial spin labeling (ASL) MRI, (Wintermark et al., 2005) are techniques that offer more direct measures of resting brain activation patterns than BOLD-based ALFF. These techniques track perfusion in the brain by measuring dynamic concentrations of a tracing agent. PET and SPECT use exogenous tracers composed of different types of radioactive contrast agents (Carroll et al., 2002), whereas ASL uses the

magnetic properties of hydrogen atoms in arterial water molecules as endogenous tracers (T. Liu, 2015). All three methods are designed to capture physiological metabolic activity correlates in the brain, such as resting cerebral blood flow (rCBF). Theoretically, CBF delivers and replenishes metabolites in activated regions; this process suggests a close association between rCBF and neuronal activity, putatively referred to as neurovascular coupling.

PET and SPECT have been used extensively to identify rCBF abnormalities associated with OCD (Alptekin et al., 2001; Busatto et al., 2000; Diler et al., 2004; Hansen et al., 2002; Harris et al., 1994; Karadağ et al., 2013; Lacerda et al., 2003; Lucey et al., 1995; Nakatani et al., 2003; Perani et al., 1995; Rubin et al., 1992; Swedo et al., 1989). Findings are inconsistent across studies but are in keeping with the CSTC circuit model of OCD and many BOLD studies. Specifically, PET- and SPECT-based measures of rCBF generally suggest that OCD is associated with perfusion abnormalities in the mPFC, cingulate, striatum, and thalamus, though directionality varies dramatically across ROIs and studies. PET and SPECT studies suggest that, compared to non-clinical controls, OCD may be associated with hyperperfusion in the lOFC (Alptekin et al., 2001; Rubin et al., 1992), medial superior frontal gyrus (Harris et al., 1994), rostral ACC, medial cingulate cortex (mCC), and posterior cingulate cortex (PCC) (Diler et al., 2004; Perani et al., 1995; Swedo et al., 1989), bilateral caudate, (Diler et al., 2004; Nakatani et al., 2003), thalamus (Alptekin et al., 2001; Lacerda et al., 2003), dorsal parietal cortex (Rubin et al., 1992), left frontotemporal cortex (Alptekin et al., 2001), and cerebellum (Busatto et al., 2000; Harris et al., 1994). However, other PET and SPECT research suggests that OCD may also be associated with hypoperfusion in the lOFC (Busatto et

al., 2000), bilateral superior frontal gyrus (Lucey et al., 1995), dorsal ACC and PCC (Busatto et al., 2000; Karadağ et al., 2013), bilateral and right caudate, (Lacerda et al., 2003; Lucey et al., 1995; Rubin et al., 1992), thalamus (Lucey et al., 1995), left and central parietal cortex (Karadağ et al., 2013; Lucey et al., 1995), and left temporal and medial superior temporal cortex (Karadağ et al., 2013; Lucey et al., 1995), as well as the inferior frontal gyrus (Karadağ et al., 2013; Lacerda et al., 2003; Lucey et al., 1995), and occipital cortex (Harris et al., 1994; Karadağ et al., 2013).

1.3   Arterial Spin Labeling

Unlike PET and SPECT, ASL uses arterial water as an endogenous tracer to track blood perfusion (T. Liu, 2015). Two image types are acquired with ASL: control images and labeled images. The control images of the brain are acquired initially, then protons within the hydrogen atom of water molecules are labeled by disrupting their aligned magnetic state with a sequence of radiofrequency interference pulses (T. Liu, 2015). As the arterial water molecules travel from feeding arteries to the capillary bed, where they will diffuse into the parenchyma, additional images are taken (T. Liu, 2015). The difference between labeled and control images is proportional to rCBF, or perfusion (T. Liu, 2015), measured in units of ml 100 g-1 per min-1 (Detre & Wang, 2002).

Three main classes of ASL exist: (1) pulsed ASL (pASL), (2) continuous ASL (CASL), and (3) velocity-selective ASL (VS-ASL) (T. Liu, 2015). pASL inverts the blood water magnetization in tissue proximal to areas of interest using short radiofrequency pulses, which can help minimize the magnetization transfer effects found in CASL (Wolff & Balaban, 1989). CASL inverts the blood water magnetization at the carotid level with a continuous pulse of RF (Wintermark et al., 2005; Zaharchuk et al.,

1999). VS-ASL is relatively new and involves selectively inverting the blood magnetization based on its velocity (Duhamel et al., 2003; Norris & Schwarzbauer, 1999; Wintermark et al., 2005).

PET and SPECT can be inexpedient due the invasiveness of the procedures (e.g., need for radioactive tracers, costliness, and longer duration needed between exams; Wintermark et al., 2005). ASL imaging procedures do not require exogenous radiotracers and can be repeated several times with no downtime necessary, which can boost the signal-to-noise ratio (SNR) and spatial resolution (PET/SPECT = 4-6 mm; ASL = 2mm; A. P. Fan et al., 2016; Wintermark et al., 2005). Additionally, relative to BOLD-based measures of resting blood flow like ALFF, ASL demonstrates decreased intrasubject variability (e.g., <10% change rescanning the same subject with ASL; Floyd et al., 2001; Parkes et al., 2004), decreased inter-subject variability during low frequency tasks (Wang et al., 2003), and decreased autocorrelation in perfusion signal noise (Aguirre et al., 2005). Moreover, ASL has the unique advantage of being an absolute quantification of baseline or dynamic perfusion, as opposed to the aggregate BOLD signal, and is therefore directly interpretable.

To date, ASL has only been used in two studies with OCD patients (Momosaka et al., 2020; Ota et al., 2020). In both studies, the researchers used a combination of pASL and CASL called pcASL. Relative to HCs, Ota (2020) reported that OCD patients had decreased rCBF in clusters encompassing the right PCC and lingual gyrus, right thalamus, and right hippocampus, and increased rCBF in clusters comprising the left temporal gyrus and left frontal white matter (Ota et al., 2020). Relative to HCs, Momosaka (2020) reported that OCD patients had decreased rCBF in clusters comprising

the right putamen, right frontal operculum and insula, right temporal pole, and left mCC; no increases in rCBF in OCD patients were found (Momosaka et al., 2020). In both studies, associations between OCD severity, measured using the Y-BOCS total score, and perfusion were measured, but were not significant (Momosaka et al., 2020; Ota et al., 2020).

Surprisingly, there was no overlap in regional differences reported by these two studies, despite the use of similar ASL techniques. Differences in sample characteristics may have contributed to this lack of consistency between studies. Most OCD patients in the sample used by Ota and colleagues were medicated with antidepressants or antipsychotics whereas OCD patients in the Momosaka study were drug free for at least four weeks prior to scanning. This difference in medication status is important, as pharmacologic intervention seems to increase activation and metabolic activity in regions implicated in OCD pathophysiology (Buchsbaum et al., 2006; Hendler et al., 2003; Karadağ et al., 2013). For example, antidepressants have been shown to boost activity in the anterior temporal cortex, PFC (Hendler et al., 2003), thalamus, and ACC (Karadağ et al., 2013). Similarly, antipsychotics have been shown to boost relative metabolic rate in the striatum, ACC, PFC, and thalamus (Buchsbaum et al., 2006) in OCD patients. Because Ota (2020) included participants taking antidepressants and antipsychotics, regions associated with OCD pathophysiology may have exhibited higher perfusion values than would be seen in a fully unmedicated group.

1.4   Current Study

The current study will replicate and extend the findings of Momosaka and colleagues (2020) by comparing rCBF between unmedicated OCD patients and HCs with

pASL data. Based on the results from prior rs-fMRI, PET, and SPECT studies, and the single ASL study with unmedicated OCD patients, we predict that OCD patients will demonstrate multiple abnormalities in rCBF, particularly within the CTSC and sensorimotor network

CHAPTER 2. METHODS AND MATERIALS

2.1   Data Collection

This study used data from the "Yale HCP Trio" study conducted at the Yale OCD Research Clinic from 2016-2019. Following preliminary phone screening, volunteers completed an in-person screening intake that included completion of a Yale Human Investigation Committee (HIC)-approved informed consent, a structured clinical interview for psychiatric disorders, and an MRI safety screening to determine eligibility. All participants completed the 17-item Hamilton Depression Rating Scale (HAMD-17; Hamilton, 1960). OCD patients also completed assessment of OCD and related symptoms, including the Yale Brown Obsessive-Compulsive Symptom (Y-BOCS) checklist and severity scales (Goodman, Price, Rasmussen, & Mazure, 1989; Goodman, Price, Rasmussen, Mazure, et al., 1989). Participants were then scheduled to complete a single MRI scan session (see MRI Data Acquisition) that included two identical, consecutive resting pASL sequences.

2.2   Participants

The Yale HCP Trio dataset includes data from 22 adult unmedicated OCD patients, 23 adult HCs and 8 adult patients with major depressive disorder (MDD); only OCD patients and HCs were be included in the present study. OCD patients and HCs did

not significantly differ on any assessed sociodemographic factors. See **Table 1** for participant details.

2.3 MRI Data Acquisition

Imaging was performed on a 3-Tesla Siemens Magnetom Prisma fit scanner using a 64-channel head coil. High-resolution 3-dimensional T1-weighted images were acquired using the Siemens product magnetization prepared rapid gradient echo (MPRAGE) sequence [repetition time (TR) = 2400 ms, echo time (TE) = 2.07 ms; flip angle (FA) = 8°; acquisition matrix = 64 x 64; field of view (FOV) = 256 mm; thickness = 0.80 mm; time = 13:37 min]. pASL perfusion MRI was performed using the Siemens product pASL QUIPSS II (T2TIPS) Q2T sequence (Wong et al., 1998b). 20 transverse slices were acquired in an ascending, interleaved fashion [TR = 3000 ms; TE = 26 ms; TI 0 = 700 ms; TI 1 = 1300 ms; TI 2 = 1300 ms; FA = 90°; acquisition matrix = 64 x 64; gap = 20 mm; FOV = 256 mm; thickness = 5 mm; acquisition time = 14:43 mins]. An identical pASL run was conducted immediately following the first pASL run.

2.4 Data Analytic Strategy

2.4.1 Preprocessing

MRI data were preprocessed using the Bayesian Inference for Arterial Spin Labeling MRI (BASIL) toolset (Chappell et al., 2009) Briefly, pASL datasets were co-registered using an boundary-based registration cost function before being averaged to yield a tagged, an untagged, and an M_0 volume for each participant. Quantitative rCBF maps were then calculated using the BASIL graphical user interface and command line tool, "oxford-asl" (Chappell et al., 2009). Images were corrected for motion, slice timing, and partial volume effects (Chappell et al., 2011), and grey matter masks were applied

2.4.2 ROI-Based Analyses

ROI-based analyses were conducted. Grey matter masked perfusion images were parcellated into 55 individual ROIs based on coordinates from the Harvard-Oxford cortical and subcortical structural atlas (Desikan et al., 2006; Frazier et al., 2005; Goldstein et al., 2007; Makris et al., 2006). Within each ROI, summary statistics were gathered. The statistic chosen for use in secondary analyses was the precision-weighted mean (PWM), which is a measure of mean perfusion weighted by voxelwise precision (1/standard deviation) estimates; it accounts for the confidence of the inference in the value at each voxel.

Twenty a priori ROIs were selected for analyses based on their relevance in prior ALFF/fALFF and rCBF research in OCD patients. The remaining ROIs from the Harvard-Oxford cortical and subcortical structural atlas were also analyzed for exploratory purposes. See **Table 2** for the complete list of a priori and post hoc ROIs.

2.4.3 Linear Mixed Effects Models

Separate linear mixed effects (LME) models were conducted to determine associations between study groups (HC vs. OCD patients) and PWM perfusion across pASL scan runs. Across all participants, additional LMEs were conducted to examine associations between HAMD-17 scores and PWM perfusion. For OCD patients, LMEs were also conducted to examine associations between Y-BOCS scores and PWM perfusion; separate LMEs were completed for Y-BOCS total score, obsessions score, and compulsions score.

Subject and intercept were modeled as random effects, and the scan run was modeled as a fixed effect for all LMEs. For LMEs comparing PWM perfusion between

HCs and OCD patients, Group and the Group-by-Run interaction were modeled as fixed effects. For LMEs testing associations between PWM perfusion and HAMD-17 or Y-BOCS scores, HAMD-17 or Y-BOCS scores and HAMD-17/Y-BOCS-by-Run interactions were included as fixed effects. OCD patients and HCs showed no significant differences in sociodemographic factors except for education level. However, the inclusion of education as a covariate did not significantly enhance model fit. As a result, no covariates were included in the LMEs. False discovery rate (FDR) was corrected with the Benjamini-Hochberg method (Benjamini & Hochberg, 1995). All analyses were conducted with R (v4.3.1; R Core Team, 2023).

Table 1 Sample Composition

	HC (N=23)	OCD (N=22)	Total (N=45)	p value
Sex				0.833
Female	15 (65.2%)	15 (68.2%)	30 (66.7%)	
Age				0.721
Mean (SD)	34.087 (14.135)	35.500 (12.149)	34.778 (13.071)	
Range	19.000 - 62.000	18.000 - 59.000	18.000 - 62.000	
Race				0.342
White	20 (87.0%)	19 (86.4%)	39 (86.7%)	
Education				0.018*
Mean (SD)	16.174 (2.249)	14.455 (2.425)	15.333 (2.468)	
Range	12.000 – 22.000	11.000 – 18.000	11.000 – 22.000	
HAMD-17 Total				
Mean (SD)	0.409 (0.844)	12.227 (7.642)	6.318 (8.034)	
Range	0.000 – 3.000	0.000 – 29.000	0.000-29.000	
YBOCS Total				
Mean (SD)	-	26.955 (5.057)	-	
Range	-	16.000 – 35.000	-	
YBOCS Obsessions				
Mean (SD)	-	13.500 (2.774)	-	
Range	-	6.000-18.000	-	
YBOCS Compulsions				
Mean (SD)	-	13.5911(3.014)	-	
Range	-	5.000-18.000	-	

Note. *$p \leq 0.05$.

Table 2 ROIs Selected for Analyses

A Priori	Post Hoc
Precuneus	Middle Temporal Gyrus temporooccipital part
Subcallosal Cortex	Left Cerebral Cortex
Cingulate Gyrus posterior division (PCC)	Middle Temporal Gyrus posterior division
Right Putamen	Right Cerebral Cortex
Precentral Gyrus	Middle Frontal Gyrus
Left Hippocampus	Lingual Gyrus
Right Thalamus	Angular Gyrus
Postcentral Gyrus	Lateral Occipital Cortex inferior division
Frontal Medial Cortex	Lateral Occipital Cortex superior division
Left Putamen	Superior Parietal Lobule
Left Thalamus	Temporal Pole
Right Caudate	Frontal Pole
Cingulate Gyrus anterior division (ACC)	Occipital Fusiform Gyrus
Supplementary Motor Area (SMA)	Temporal Fusiform Cortex posterior division
Orbital Frontal Cortex (OFC)	Supramarginal Gyrus anterior division
Central Opercular Cortex	Temporal Occipital Fusiform Cortex
Right Hippocampus	Occipital Pole
Insular Cortex	Inferior Temporal Gyrus temporooccipital part
Paracingulate Gyrus	Superior Frontal Gyrus
Left Caudate	

Note. The regions selected are from the Harvard-Oxford cortical and subcortical structural atlases which are probabilistic atlases covering 48 cortical and 21 subcortical structural areas. Regions are derived from structural data and segmentations, provided by the Harvard Center for Morphometric Analysis (Desikan et al., 2006; Frazier et al., 2005; Goldstein et al., 2007; Makris et al., 2006).

CHAPTER 3.   RESULTS

3.1   A Priori ROIs

In general, different measures of the same construct converged strongly. However, there was weaker convergence in some cases, particularly for the MCMI. See all bivariate correlations in Tables 1-6.

3.1.1   Effects of Group (HC vs. OCD)

The Main effects of Group suggest that PWM perfusion was higher in OCD patients than HCs in the precentral gyrus (puncorr = 0.048; pcorr = 0.478) and postcentral gyrus (puncorr = 0.024; pcorr = 0.478). Main effects of Run in the precuneus (puncorr = 0.006; pcorr = 0.086), subcallosal cortex (puncorr = 0.009; pcorr = 0.086), and the PCC (puncorr = 0.046; pcorr = 0.310) suggest that PWM perfusion increased in these regions from run 1 to run 2. Lastly, Group*Run interactions in the subcallosal cortex (puncorr = 0.03; pcorr = 0.276) and precuneus (puncorr = 0.026; pcorr = 0.276) suggest that PWM perfusion increased more in these regions from run 1 to run 2 for HCs when compared to OCD patients. None of these effects survived FDR correction. See Table 3 for a summary of all LMEs comparing HC with OCD patients.

3.1.2   Effects of HAMD-17

The main effect of HAMD-17 was not significant for any ROI. Main effects of Run in the subcallosal cortex (p_{uncorr} = 0.006; p_{corr} = 0.118), PCC (p_{uncorr} = 0.035; p_{corr} = 0.164), precuneus (p_{uncorr} = 0.038; p_{corr} = 0.164), right putamen (p_{uncorr} = 0.039; p_{corr} = 0.164), and precentral gyrus (p_{uncorr} = 0.041; p_{corr} = 0.164) suggest that PWM perfusion increased in these regions from run 1 to run 2. Lastly, HAMD-17*Run interactions in the left thalamus (p_{uncorr} = 0.011; p_{corr} = 0.081), precentral gyrus (p_{uncorr} = 0.013; p_{corr} =

0.081), subcallosal cortex ($p_{uncorr} = 0.015$; $p_{corr} = 0.081$), ACC ($p_{uncorr} = 0.02$; $p_{corr} = 0.081$), PCC ($p_{uncorr} = 0.02$; $p_{corr} = 0.081$), and the SMA ($p_{uncorr} = 0.046$; $p_{corr} = 0.081$) suggest that PWM perfusion increased more in these regions from run 1 to run 2 as HAMD-17 scores decreased. No main effects or interaction effects survived FDR correction in the HAMD-17 models. See **Table 4** for a summary of all LMEs that include HAMD-17.

3.1.3   Effects of Y-BOCS

No main effects of Y-BOCS were significant ($p_{uncorr} < .05$) in the Y-BOCS Total (**Table 5**) or Y-BOCS Compulsions (**Table 6**) models. Similarly, no Y-BOCS*Run interaction effects were significant ($p_{uncorr} < .05$) in the Y-BOCS Total, Y-BOCS Compulsions, or Y-BOCS Obsessions models. The main effect of Y-BOCS Obsessions in the precentral gyrus ($p_{uncorr} = 0.005$; $p_{corr} = 0.082$), SMA ($p_{uncorr} = 0.009$; $p_{corr} = 0.082$), ACC ($p_{uncorr} = 0.012$; $p_{corr} = 0.082$), precuneus ($p_{uncorr} = 0.03$; $p_{corr} = 0.151$), and the right hippocampus ($p_{uncorr} = 0.047$; $p_{corr} = 0.182$) suggest that PWM perfusion decreased in these regions as severity of obsessions increased (see **Figure 1** and **Table 7** for a summary of all LMEs that include Y-BOCS obsessions). None of these effects survived FDR correction, but several were significant at the $p_{uncorr} < .05$ level.

3.1.4   Post hoc analyses of Low vs. High obsessions.

Post hoc LMEs were conducted to explore the main effects of Y-BOCS Obsessions on PWM perfusion. This was accomplished by separating OCD patients into two groups using a Y-BOCS Obsessions score median-split (median = 14), resulting in three groups: Low-Obsession (n=11) and High-Obsession (n=11) OCD patients and HCs, (n=23). Separate LMEs were used to compare PWM perfusion between HCs and Low-

16

Obsession OCD patients, between HCs and High-Obsession OCD patients, and between Low- and High-Obsession OCD patients.

In the HC vs Low-Obsession models, main effects of Group in the precentral gyrus ($p_{uncorr} = 0.002$; $p_{corr} = 0.017$), postcentral gyrus ($p_{uncorr} = 0.001$; $p_{corr} = 0.017$), ACC ($p_{uncorr} = 0.01$; $p_{corr} = 0.070$), SMA ($p_{uncorr} = 0.015$; $p_{corr} = 0.077$), paracingulate gyrus ($p_{uncorr} = 0.034$; $p_{corr} = 0.116$), precuneus ($p_{uncorr} = 0.04$; $p_{corr} = 0.116$), central operculum ($p_{uncorr} = 0.043$; $p_{corr} = 0.116$), and insula ($p_{uncorr} = 0.046$; $p_{corr} = 0.116$) suggested that PWM perfusion in these regions was higher in Low-Obsession OCD patients than HCs. Main effect of Run in the subcallosal cortex ($p_{uncorr} = 0.007$; $p_{corr} = 0.119$) and precuneus ($p_{uncorr} = 0.012$; $p_{corr} = 0.119$), suggested that PWM perfusion in these regions increased from run 1 to run 2 among HCs and patients with less severe obsessions. Lastly, Group*Run interactions in the subcallosal cortex ($p_{uncorr} = 0.008$; $p_{corr} = 0.158$) suggest that PWM perfusion increased more in this region from run 1 to run 2 for HCs when compared to participants with lower severity of obsessions. The main effect of Group in the precentral and postcentral gyri were the only effects that survived FDR correction ($p_{corr} = 0.017$) in the HC vs. Low-Obsession models (see **Figure 2** and **Table 8** for a summary of all LMEs comparing HCs and Low-Obsession OCD patients).

In the HC vs High-Obsession models, the main effect of Group and Group*Run interaction were not significant ($p_{uncorr} < 0.05$) for any ROIs. However, the main effect of Run in the precuneus ($p_{uncorr} = 0.007$; $p_{corr} = 0.114$), subcallosal cortex ($p_{uncorr} = 0.011$; $p_{corr} = 0.114$), PCC ($p_{uncorr} = 0.034$; $p_{corr} = 0.216$), and right putamen ($p_{uncorr} = 0.043$; $p_{corr} = 0.216$) suggests that PWM perfusion increased in these regions from run 1 to run 2.

None of these effects survived FDR correction. See **Table 9** for a summary of all LMEs comparing HCs and High-Obsession OCD patients).

In the Low- vs. High-Obsession models, main effects of Group in the precentral gyrus (p_{uncorr} = 0.004; p_{corr} = 0.088), postcentral gyrus (p_{uncorr} = 0.018; p_{corr} = 0.116), ACC (p_{uncorr} = 0.014; p_{corr} = 0.116), SMA (p_{uncorr} = 0.023; p_{corr} = 0.116), and insula (p_{uncorr} = 0.044; p_{corr} = 0.174), suggested that PWM perfusion in these regions was higher in Low-Obsession OCD patients than High-Obsession OCD patients. However, none of these effects survived FDR correction. The Run and Group*Run effects were not significant (p_{uncorr} < 0.05) for any ROIs. See **Table 10** for a summary of all LMEs comparing Low-Obsession and High-Obsession OCD patients)..

3.2 Exploratory ROIs

3.2.1 Effects of Group (HC vs. OCD)

Among post hoc ROIs, the main effect of Group in the superior parietal lobule (p_{uncorr} = 0.038; p_{corr} = 0.478) suggested that PWM perfusion was higher in OCD patients than HC. The Group*Run interaction in the middle frontal gyrus (p_{uncorr} = 0.027; p_{corr} = 0.388) suggested that PWM perfusion increased more from run 1 to run 2 in this region for HCs when compared to OCD patients. Neither of these effects survived FDR correction.

3.2.2 Effects of HAMD-17

Among post hoc ROIs, no main effects or interaction effects were significant (p_{uncorr} < 0.05) in the HAMD-17 models.

3.2.3 Effects of Y-BOCS

Among post hoc ROIs the main effect of Y-BOCS Obsessions in the posterior middle temporal gyrus ($p_{uncorr} = 0.01$; $p_{corr} = 0.096$), anterior supramarginal gyrus ($p_{uncorr} = 0.013$; $p_{corr} = 0.096$), left cerebral cortex ($p_{uncorr} = 0.015$; $p_{corr} = 0.096$), and right cerebral cortex ($p_{uncorr} = 0.038$; $p_{corr} = 0.184$) suggested that PWM perfusion decreased in these regions as severity of obsessions increased. None of these Y-BOCS Obsession main effects survived FDR correction.

3.2.4 Post hoc Analyses of Low vs. High Obsessions.

Among post hoc ROIs comparing HCs with the Low-Obsession group, the main effect of Group in the superior parietal lobule ($p_{uncorr} = 0.006$; $p_{corr} = 0.074$), posterior middle temporal gyrus ($p_{uncorr} = 0.008$; $p_{corr} = 0.074$), superior frontal gyrus ($p_{uncorr} = 0.018$; $p_{corr} = 0.097$), left cerebral cortex ($p_{uncorr} = 0.02$; $p_{corr} = 0.097$), lateral superior occipital cortex ($p_{uncorr} = 0.032$; $p_{corr} = 0.120$), right cerebral cortex ($p_{uncorr} = 0.043$; $p_{corr} = 0.120$), and frontal pole ($p_{uncorr} = 0.043$; $p_{corr} = 0.120$) suggest that PWM perfusion in these regions was higher in Low-Obsession OCD patients than HCs. Additionally, the main effects of Run and Low-Obsession Group*Run interaction effects were not significant ($p_{uncorr} < 0.05$). No main effects or interaction effects survived FDR correction, but several were significant at the $p_{corr} < .10$ level.

Among post hoc ROIs comparing HCs with the High-Obsession group, no Group or Group*Run effects were significant ($p_{uncorr} < 0.05$). The main effect of Run in the middle temporal gyrus ($p_{uncorr} = 0.043$; $p_{corr} = 0.337$) suggested that PWM perfusion increased from run 1 to run 2 in this region. This effect did not survive FDR correction.

Among post hoc ROIs comparing Low-Obsession OCD patients with the High-Obsession OCD patient group, main effects of Group in the left cerebral cortex ($p_{uncorr} = 0.028$; $p_{corr} = 0.183$), superior frontal gyrus ($p_{uncorr} = 0.029$; $p_{corr} = 0.183$), superior parietal lobule ($p_{uncorr} = 0.041$; $p_{corr} = 0.183$), anterior middle temporal gyrus ($p_{uncorr} = 0.044$; $p_{corr} = 0.183$), and posterior middle temporal gyrus ($p_{uncorr} = 0.049$; $p_{corr} = 0.183$), suggested that PWM perfusion in these regions was higher in Low-Obsession OCD patients than High-Obsession OCD patients. None of these effects survived FDR correction. The main effect of Run and Group*Run interaction were not significant ($p_{uncorr} < 0.05$) for any ROIs.

Table 3 Group (HC vs. OCD) Effects on PWM Perfusion Across A Priori ROI

ROI	Variable	B/F	SE	df	p	95% CI
Central Opercular Cortex						
	Intercept	44.86	1.96	43	0.000	[40.91, 48.82]
	Group	4.17	2.81	43	0.144	[-1.49, 9.84]
	Run	0.95	1.26	43	0.457	[-1.6, 3.5]
	Group:Run	-2.52	1.81	43	0.171	[-6.17, 1.13]
Anterior Cingulate						
	Intercept	46.51	2.01	43	0.000	[42.46, 50.55]
	Group	3.57	2.87	43	0.221	[-2.22, 9.35]
	Run	0.92	1.05	43	0.388	[-1.2, 3.03]
	Group:Run	-2.55	1.50	43	0.096	[-5.58, 0.48]
Posterior Cingulate						
	Intercept	45.28	2.43	43	0.000	[40.38, 50.17]
	Group	0.43	3.47	43	0.901	[-6.57, 7.44]
	Run	2.77	1.35	43	0.046*	[0.05, 5.49]
	Group:Run	-3.45	1.93	43	0.081	[-7.34, 0.44]
Frontal Medial Cortex						
	Intercept	32.18	2.39	43	0.000	[27.37, 37]
	Group	2.24	3.41	43	0.516	[-4.65, 9.12]
	Run	2.01	1.68	43	0.237	[-1.37, 5.39]
	Group:Run	-3.33	2.40	43	0.172	[-8.16, 1.51]
Frontal Orbital Cortex						
	Intercept	33.40	1.74	43	0.000	[29.89, 36.92]
	Group	1.66	2.49	43	0.510	[-3.37, 6.69]
	Run	0.96	1.34	43	0.477	[-1.74, 3.67]
	Group:Run	-1.68	1.92	43	0.387	[-5.55, 2.19]
Insula						
	Intercept	36.19	1.50	43	0.000	[33.17, 39.21]
	Group	2.90	2.14	43	0.183	[-1.42, 7.22]
	Run	0.54	1.04	43	0.605	[-1.56, 2.65]
	Group:Run	-1.35	1.49	43	0.370	[-4.36, 1.66]
Left Caudate						
	Intercept	33.58	2.02	43	0.000	[29.51, 37.64]
	Group	1.46	2.88	43	0.616	[-4.35, 7.27]
	Run	0.17	0.79	43	0.831	[-1.43, 1.77]
	Group:Run	0.27	1.14	43	0.811	[-2.02, 2.57]
Left Hippocampus						
	Intercept	35.82	1.84	43	0.000	[32.11, 39.52]
	Group	-0.82	2.63	43	0.755	[-6.12, 4.47]
	Run	2.04	1.22	43	0.103	[-0.43, 4.51]
	Group:Run	-3.27	1.75	43	0.069	[-6.8, 0.26]
Left Putamen						
	Intercept	51.75	2.69	43	0.000	[46.33, 57.17]

Table 3 (continued)

	Group	0.51	3.85	43	0.895	[-7.24, 8.26]
	Run	1.44	1.29	43	0.271	[-1.16, 4.03]
	Group:Run	0.31	1.84	43	0.867	[-3.41, 4.03]
Left Thalamus						
	Intercept	56.19	3.47	43	0.000	[49.19, 63.19]
	Group	-0.69	4.97	43	0.889	[-10.71, 9.32]
	Run	1.63	1.51	43	0.287	[-1.42, 4.67]
	Group:Run	-4.00	2.16	43	0.071	[-8.36, 0.35]
Paracingulate						
	Intercept	44.73	2.33	43	0.000	[40.02, 49.44]
	Group	4.13	3.34	43	0.222	[-2.6, 10.87]
	Run	0.54	1.18	43	0.651	[-1.84, 2.92]
	Group:Run	-1.91	1.69	43	0.265	[-5.31, 1.5]
Postcentral Gyrus						
	Intercept	36.19	2.47	43	0.000	[31.21, 41.16]
	Group	8.25	3.53	43	0.024*	[1.13, 15.36]
	Run	1.73	1.19	43	0.152	[-0.67, 4.13]
	Group:Run	-1.38	1.70	43	0.422	[-4.81, 2.05]
Precentral Gyrus						
	Intercept	40.27	2.42	43	0.000	[35.39, 45.14]
	Group	7.05	3.46	43	0.048*	[0.07, 14.03]
	Run	2.38	1.27	43	0.068	[-0.18, 4.95]
	Group:Run	-3.16	1.82	43	0.090	[-6.84, 0.51]
Precuneous						
	Intercept	37.81	2.15	43	0.000	[33.49, 42.14]
	Group	4.08	3.07	43	0.191	[-2.11, 10.26]
	Run	2.41	0.84	43	0.006*	[0.72, 4.11]
	Group:Run	-2.77	1.20	43	0.026*	[-5.2, -0.34]
Right Caudate						
	Intercept	33.64	1.95	43	0.000	[29.69, 37.58]
	Group	2.01	2.80	43	0.476	[-3.63, 7.65]
	Run	1.26	1.03	43	0.228	[-0.82, 3.35]
	Group:Run	-1.22	1.48	43	0.415	[-4.19, 1.76]
Right Hippocampus						
	Intercept	36.20	1.70	43	0.000	[32.77, 39.63]
	Group	-1.58	2.43	43	0.520	[-6.49, 3.33]
	Run	0.79	1.07	43	0.464	[-1.37, 2.96]
	Group:Run	-0.69	1.54	43	0.654	[-3.8, 2.41]
Right Putamen						
	Intercept	50.18	2.31	43	0.000	[45.52, 54.85]
	Group	1.25	3.31	43	0.707	[-5.42, 7.93]
	Run	2.29	1.43	43	0.118	[-0.61, 5.18]
	Group:Run	-0.57	2.05	43	0.782	[-4.71, 3.57]
Right Thalamus						
	Intercept	54.50	3.16	43	0.000	[48.13, 60.87]

Table 3 (continued)

	Group	-0.98	4.52	43	0.830	[-10.09, 8.14]
	Run	1.98	1.49	43	0.190	[-1.02, 4.97]
	Group:Run	-3.20	2.12	43	0.140	[-7.48, 1.09]
Supplementary Motor Area						
	Intercept	38.08	1.88	43	0.000	[34.29, 41.88]
	Group	3.70	2.69	43	0.176	[-1.72, 9.12]
	Run	1.17	1.34	43	0.390	[-1.54, 3.87]
	Group:Run	-2.79	1.92	43	0.153	[-6.66, 1.08]
Subcallosal Cortex						
	Intercept	33.28	2.01	43	0.000	[29.23, 37.33]
	Group	-5.08	2.87	43	0.084	[-10.87, 0.71]
	Run	2.53	0.92	42	0.009*	[0.68, 4.39]
	Group:Run	-2.92	1.30	42	0.030*	[-5.55, -0.3]

Note. *p_{uncorr} < .05, **p_{corr} < .05.

Table 4 HAMD-17 Severity Score Effects on PWM Perfusion Across A Priori ROI

ROI	Variable	B/F	SE	df	p	95% CI
Central Opercular Cortex						
	Intercept	45.09	1.78	42	0.000	[41.49, 48.69]
	hamd17	0.24	0.18	42	0.176	[-0.11, 0.59]
	Run	0.94	1.16	42	0.419	[-1.39, 3.28]
	hamd17:Run	-0.21	0.11	42	0.076	[-0.44, 0.02]
Anterior Cingulate						
	Intercept	47.21	1.83	42	0.000	[43.51, 50.9]
	hamd17	0.13	0.18	42	0.472	[-0.23, 0.49]
	Run	0.85	0.92	42	0.360	[-1, 2.7]
	hamd17:Run	-0.22	0.09	42	0.020*	[-0.4, -0.04]
Posterior Cingulate						
	Intercept	44.85	2.20	42	0.000	[40.42, 49.29]
	hamd17	0.06	0.22	42	0.768	[-0.37, 0.5]
	Run	2.55	1.17	42	0.035*	[0.19, 4.91]
	hamd17:Run	-0.28	0.11	42	0.020*	[-0.51, -0.05]
Frontal Medial Cortex						
	Intercept	33.15	2.23	42	0.000	[28.65, 37.65]
	hamd17	0.03	0.22	42	0.881	[-0.41, 0.47]
	Run	0.79	1.58	42	0.619	[-2.4, 3.98]
	hamd17:Run	-0.09	0.16	42	0.576	[-0.4, 0.23]
Frontal Orbital Cortex						
	Intercept	34.05	1.63	42	0.000	[30.76, 37.33]
	hamd17	0.04	0.16	42	0.811	[-0.28, 0.36]
	Run	0.51	1.26	42	0.689	[-2.03, 3.05]
	hamd17:Run	-0.06	0.12	42	0.623	[-0.31, 0.19]
Insula						
	Intercept	36.39	1.39	42	0.000	[33.6, 39.19]
	hamd17	0.19	0.14	42	0.181	[-0.09, 0.46]
	Run	0.66	0.93	42	0.484	[-1.22, 2.54]
	hamd17:Run	-0.15	0.09	42	0.112	[-0.33, 0.04]
Left Caudate						
	Intercept	33.54	1.86	42	0.000	[29.8, 37.29]
	hamd17	0.09	0.18	42	0.640	[-0.28, 0.45]
	Run	0.66	0.73	42	0.368	[-0.8, 2.13]
	hamd17:Run	-0.07	0.07	42	0.338	[-0.21, 0.07]
Left Hippocampus						
	Intercept	35.28	1.72	42	0.000	[31.81, 38.74]
	hamd17	0.00	0.17	42	0.991	[-0.34, 0.34]
	Run	1.81	1.14	42	0.120	[-0.49, 4.11]
	hamd17:Run	-0.20	0.11	42	0.076	[-0.43, 0.02]
Left Putamen						
	Intercept	52.60	2.49	42	0.000	[47.58, 57.62]
	hamd17	-0.11	0.24	42	0.666	[-0.6, 0.39]
	Run	2.25	1.18	42	0.063	[-0.13, 4.64]

Table 4 (continued)

	hamd17:Run	-0.12 0.12	42	0.305	[-0.35, 0.11]
Left Thalamus					
	Intercept	55.44 3.07	42	0.000	[49.24, 61.63]
	hamd17	-0.04 0.30	42	0.903	[-0.65, 0.57]
	Run	1.67 1.33	42	0.216	[-1.02, 4.37]
	hamd17:Run	-0.35 0.13	42	0.011*	[-0.61, -0.08]
Paracingulate					
	Intercept	45.24 2.14	42	0.000	[40.93, 49.54]
	hamd17	0.20 0.21	42	0.343	[-0.22, 0.62]
	Run	0.34 1.05	42	0.747	[-1.78, 2.47]
	hamd17:Run	-0.15 0.10	42	0.152	[-0.36, 0.06]
Postcentral Gyrus					
	Intercept	37.57 2.34	42	0.000	[32.84, 42.3]
	hamd17	0.41 0.23	42	0.082	[-0.05, 0.87]
	Run	1.74 1.06	42	0.107	[-0.39, 3.88]
	hamd17:Run	-0.14 0.10	42	0.179	[-0.35, 0.07]
Precentral Gyrus					
	Intercept	41.06 2.24	42	0.000	[36.54, 45.57]
	hamd17	0.40 0.22	42	0.079	[-0.05, 0.84]
	Run	2.28 1.08	42	0.041*	[0.1, 4.47]
	hamd17:Run	-0.28 0.11	42	0.013*	[-0.49, -0.06]
Precuneous					
	Intercept	39.05 1.97	42	0.000	[35.07, 43.04]
	hamd17	0.08 0.19	42	0.669	[-0.31, 0.47]
	Run	1.67 0.78	42	0.038*	[0.1, 3.23]
	hamd17:Run	-0.12 0.08	42	0.114	[-0.28, 0.03]
Right Caudate					
	Intercept	34.02 1.78	42	0.000	[30.42, 37.61]
	hamd17	0.05 0.17	42	0.780	[-0.3, 0.4]
	Run	1.64 0.94	42	0.089	[-0.26, 3.53]
	hamd17:Run	-0.16 0.09	42	0.099	[-0.34, 0.03]
Right Hippocampus					
	Intercept	36.22 1.56	42	0.000	[33.07, 39.37]
	hamd17	-0.15 0.15	42	0.325	[-0.46, 0.16]
	Run	0.56 1.00	42	0.579	[-1.47, 2.59]
	hamd17:Run	-0.02 0.10	42	0.841	[-0.22, 0.18]
Right Putamen					
	Intercept	50.69 2.14	42	0.000	[46.37, 55.02]
	hamd17	0.00 0.21	42	0.997	[-0.42, 0.43]
	Run	2.79 1.31	42	0.039*	[0.14, 5.43]
	hamd17:Run	-0.14 0.13	42	0.273	[-0.4, 0.12]
Right Thalamus					
	Intercept	54.30 2.79	42	0.000	[48.66, 59.93]
	hamd17	-0.12 0.27	42	0.663	[-0.67, 0.43]
	Run	1.41 1.30	42	0.284	[-1.21, 4.02]
	hamd17:Run	-0.21 0.13	42	0.101	[-0.47, 0.04]

Table 4 (continued)

Supplementary Motor Area

Intercept	38.55	1.70	42	0.000	[35.13, 41.97]
hamd17	0.19	0.17	42	0.265	[-0.15, 0.52]
Run	0.92	1.15	42	0.426	[-1.39, 3.23]
hamd17:Run	-0.23	0.11	42	0.046*	[-0.46, 0]

Subcallosal Cortex

Intercept	32.27	1.90	42	0.000	[28.43, 36.1]
hamd17	-0.20	0.19	42	0.292	[-0.58, 0.18]
Run	2.44	0.84	41	0.006*	[0.74, 4.14]
hamd17:Run	-0.21	0.08	41	0.015*	[-0.37, -0.04]

Note. *$p_{uncorr} < .05$, **$p_{corr} < .05$.

Table 5 Y-BOCS Total Severity Score Effects On PWM Perfusion Across A Priori ROI

ROI	Variable	B/F	SE	df	p	95% CI
Central Opercular Cortex						
	Intercept	43.74	11.04	20	0.001	[20.7, 66.77]
	Run	7.05	8.67	20	0.426	[-11.04, 25.13]
	ybocs_tot	0.20	0.40	20	0.631	[-0.64, 1.04]
	ybocs_tot:Run	-0.32	0.32	20	0.324	[-0.98, 0.34]
Anterior Cingulate						
	Intercept	62.80	12.36	20	0.000	[37.02, 88.58]
	Run	-3.63	6.90	20	0.604	[-18.02, 10.75]
	ybocs_tot	-0.47	0.45	20	0.307	[-1.41, 0.47]
	ybocs_tot:Run	0.07	0.25	20	0.772	[-0.45, 0.6]
Posterior Cingulate						
	Intercept	31.33	14.66	20	0.045	[0.75, 61.9]
	Run	4.22	8.64	20	0.630	[-13.79, 22.24]
	ybocs_tot	0.53	0.53	20	0.330	[-0.58, 1.65]
	ybocs_tot:Run	-0.18	0.32	20	0.570	[-0.84, 0.48]
Frontal Medial Cortex						
	Intercept	38.12	13.99	20	0.013	[8.94, 67.3]
	Run	-7.49	11.57	20	0.525	[-31.62, 16.64]
	ybocs_tot	-0.14	0.51	20	0.791	[-1.2, 0.93]
	ybocs_tot:Run	0.23	0.42	20	0.594	[-0.65, 1.11]
Frontal Orbital Cortex						
	Intercept	43.60	10.57	20	0.001	[21.55, 65.65]
	Run	2.67	9.71	20	0.787	[-17.6, 22.93]
	ybocs_tot	-0.32	0.39	20	0.421	[-1.12, 0.49]
	ybocs_tot:Run	-0.13	0.35	20	0.727	[-0.86, 0.61]
Insula						
	Intercept	40.14	7.47	20	0.000	[24.55, 55.73]
	Run	2.02	6.95	20	0.775	[-12.49, 16.52]
	ybocs_tot	-0.04	0.27	20	0.888	[-0.61, 0.53]
	ybocs_tot:Run	-0.10	0.25	20	0.684	[-0.63, 0.42]
Left Caudate						
	Intercept	34.85	11.89	20	0.008	[10.05, 59.65]
	Run	4.28	5.20	20	0.420	[-6.56, 15.13]
	ybocs_tot	0.01	0.43	20	0.988	[-0.9, 0.91]
	ybocs_tot:Run	-0.14	0.19	20	0.462	[-0.54, 0.25]
Left Hippocampus						
	Intercept	35.96	8.19	20	0.000	[18.88, 53.04]
	Run	11.66	7.00	20	0.111	[-2.93, 26.25]
	ybocs_tot	-0.04	0.30	20	0.905	[-0.66, 0.59]
	ybocs_tot:Run	-0.48	0.26	20	0.076	[-1.01, 0.05]
Left Putamen						
	Intercept	70.30	13.87	20	0.000	[41.37, 99.23]
	Run	9.30	8.62	20	0.294	[-8.69, 27.29]
	ybocs_tot	-0.67	0.51	20	0.201	[-1.72, 0.39]

Table 5 (continued)

	ybocs_tot:Run	-0.28	0.31	20	0.384	[-0.94, 0.38]

Left Thalamus

Intercept	49.16	18.75	20	0.016	[10.04, 88.28]
Run	3.81	10.28	20	0.715	[-17.64, 25.26]
ybocs_tot	0.23	0.68	20	0.735	[-1.19, 1.66]
ybocs_tot:Run	-0.23	0.38	20	0.548	[-1.01, 0.55]

Paracingulate

Intercept	56.30	14.53	20	0.001	[26, 86.6]
Run	-3.55	8.23	20	0.671	[-20.72, 13.62]
ybocs_tot	-0.28	0.53	20	0.608	[-1.38, 0.83]
ybocs_tot:Run	0.08	0.30	20	0.790	[-0.55, 0.71]

Postcentral Gyrus

Intercept	43.44	16.27	19	0.015	[9.38, 77.5]
Run	-2.99	7.33	19	0.687	[-18.33, 12.34]
ybocs_tot	-0.02	0.58	19	0.974	[-1.24, 1.2]
ybocs_tot:Run	0.10	0.26	19	0.704	[-0.45, 0.65]

Precentral Gyrus

Intercept	63.61	14.95	20	0.000	[32.43, 94.79]
Run	-0.49	7.47	20	0.948	[-16.08, 15.1]
ybocs_tot	-0.60	0.55	20	0.281	[-1.74, 0.53]
ybocs_tot:Run	-0.01	0.27	20	0.969	[-0.58, 0.56]

Precuneous

Intercept	54.03	12.79	20	0.000	[27.34, 80.72]
Run	-1.17	4.51	20	0.797	[-10.58, 8.23]
ybocs_tot	-0.45	0.47	20	0.346	[-1.42, 0.52]
ybocs_tot:Run	0.03	0.16	20	0.855	[-0.31, 0.37]

Right Caudate

Intercept	40.86	10.23	20	0.001	[19.52, 62.2]
Run	4.85	6.56	20	0.468	[-8.84, 18.54]
ybocs_tot	-0.19	0.37	20	0.610	[-0.97, 0.59]
ybocs_tot:Run	-0.18	0.24	20	0.465	[-0.68, 0.32]

Right Hippocampus

Intercept	48.42	8.90	20	0.000	[29.86, 66.99]
Run	7.66	6.92	20	0.282	[-6.77, 22.08]
ybocs_tot	-0.51	0.32	20	0.131	[-1.19, 0.17]
ybocs_tot:Run	-0.28	0.25	20	0.280	[-0.81, 0.25]

Right Putamen

Intercept	62.04	11.80	20	0.000	[37.42, 86.67]
Run	2.69	10.45	20	0.799	[-19.1, 24.48]
ybocs_tot	-0.39	0.43	20	0.372	[-1.29, 0.51]
ybocs_tot:Run	-0.04	0.38	20	0.925	[-0.83, 0.76]

Right Thalamus

Intercept	50.34	17.42	20	0.009	[14.01, 86.67]
Run	-7.55	9.43	20	0.433	[-27.22, 12.13]
ybocs_tot	0.12	0.64	20	0.855	[-1.21, 1.44]
ybocs_tot:Run	0.23	0.34	20	0.503	[-0.48, 0.95]

Table 5 (continued)

Supplementary Motor Area

Intercept	52.45	11.36	20	0.000	[28.76, 76.15]
Run	-9.96	7.92	20	0.223	[-26.48, 6.56]
ybocs_tot	-0.40	0.41	20	0.351	[-1.26, 0.47]
ybocs_tot:Run	0.31	0.29	20	0.297	[-0.29, 0.91]

Subcallosal Cortex

Intercept	34.20	9.77	20	0.002	[13.81, 54.59]
Run	-0.89	5.20	20	0.866	[-11.73, 9.95]
ybocs_tot	-0.22	0.36	20	0.540	[-0.97, 0.52]
ybocs_tot:Run	0.02	0.19	20	0.923	[-0.38, 0.41]

Note. *$p_{uncorr} < .05$, **$p_{corr} < .05$.

Table 6 Y-BOCS Compulsion Severity Sub-Score Effects On PWM Perfusion Across A Priori ROI

ROI	Variable	B/F	SE	df	p	95% CI
Central Opercular Cortex						
	Intercept	33.76	8.94	20	0.001	[15.12, 52.4]
	Run	7.00	7.22	20	0.344	[-8.06, 22.06]
	ybocs_cmp	1.12	0.64	20	0.095	[-0.22, 2.46]
	ybocs_cmp:Run	-0.63	0.52	20	0.239	[-1.71, 0.45]
Anterior Cingulate						
	Intercept	46.99	10.61	20	0.000	[24.85, 69.13]
	Run	-2.68	5.81	20	0.650	[-14.81, 9.44]
	ybocs_cmp	0.23	0.76	20	0.769	[-1.36, 1.82]
	ybocs_cmp:Run	0.08	0.42	20	0.856	[-0.79, 0.95]
Posterior Cingulate						
	Intercept	27.54	12.01	20	0.033	[2.49, 52.58]
	Run	3.86	7.26	20	0.600	[-11.27, 19]
	ybocs_cmp	1.34	0.86	20	0.137	[-0.46, 3.14]
	ybocs_cmp:Run	-0.33	0.52	20	0.529	[-1.42, 0.75]
Frontal Medial Cortex						
	Intercept	31.29	11.69	20	0.014	[6.91, 55.67]
	Run	-7.37	9.71	20	0.457	[-27.63, 12.89]
	ybocs_cmp	0.23	0.84	20	0.786	[-1.52, 1.98]
	ybocs_cmp:Run	0.45	0.70	20	0.531	[-1.01, 1.9]
Frontal Orbital Cortex						
	Intercept	37.54	9.06	20	0.001	[18.63, 56.44]
	Run	2.44	8.17	20	0.768	[-14.6, 19.49]
	ybocs_cmp	-0.18	0.65	20	0.783	[-1.54, 1.18]
	ybocs_cmp:Run	-0.23	0.59	20	0.697	[-1.46, 0.99]
Insula						
	Intercept	31.88	6.18	20	0.000	[18.98, 44.78]
	Run	3.25	5.81	20	0.582	[-8.86, 15.36]
	ybocs_cmp	0.53	0.44	20	0.247	[-0.4, 1.46]
	ybocs_cmp:Run	-0.30	0.42	20	0.482	[-1.17, 0.57]
Left Caudate						
	Intercept	29.50	9.98	20	0.008	[8.69, 50.31]
	Run	3.78	4.37	20	0.398	[-5.34, 12.9]
	ybocs_cmp	0.41	0.72	20	0.576	[-1.09, 1.9]
	ybocs_cmp:Run	-0.25	0.31	20	0.444	[-0.9, 0.41]
Left Hippocampus						
	Intercept	29.05	7.03	20	0.001	[14.39, 43.72]
	Run	10.00	5.84	20	0.103	[-2.19, 22.19]
	ybocs_cmp	0.44	0.51	20	0.397	[-0.62, 1.49]
	ybocs_cmp:Run	-0.83	0.42	20	0.063	[-1.7, 0.05]
Left Putamen						
	Intercept	59.14	12.29	20	0.000	[33.5, 84.77]
	Run	3.62	7.39	20	0.629	[-11.79, 19.04]

Table 6 (continued)

	ybocs_cmp	-0.51	0.88	20	0.573	[-2.35, 1.34]
	ybocs_cmp:Run	-0.14	0.53	20	0.798	[-1.25, 0.97]

Left Thalamus

Intercept	43.61	15.64	20	0.011	[10.98, 76.24]
Run	1.90	8.68	20	0.829	[-16.21, 20.01]
ybocs_cmp	0.87	1.12	20	0.446	[-1.47, 3.22]
ybocs_cmp:Run	-0.31	0.62	20	0.619	[-1.62, 0.99]

Paracingulate

Intercept	42.86	12.14	20	0.002	[17.53, 68.19]
Run	-5.45	6.88	20	0.438	[-19.8, 8.9]
ybocs_cmp	0.44	0.87	20	0.619	[-1.38, 2.26]
ybocs_cmp:Run	0.30	0.49	20	0.551	[-0.73, 1.33]

Postcentral Gyrus

Intercept	41.22	14.41	20	0.010	[11.16, 71.27]
Run	3.70	5.80	20	0.531	[-8.39, 15.78]
ybocs_cmp	0.24	1.04	20	0.822	[-1.92, 2.4]
ybocs_cmp:Run	-0.25	0.42	20	0.561	[-1.11, 0.62]

Precentral Gyrus

Intercept	42.67	12.93	20	0.004	[15.7, 69.64]
Run	-0.74	6.29	20	0.907	[-13.87, 12.38]
ybocs_cmp	0.34	0.93	20	0.717	[-1.6, 2.28]
ybocs_cmp:Run	0.00	0.45	20	0.995	[-0.95, 0.94]

Precuneous

Intercept	40.35	10.99	20	0.002	[17.43, 63.27]
Run	-1.96	3.78	20	0.609	[-9.85, 5.92]
ybocs_cmp	0.11	0.79	20	0.888	[-1.53, 1.76]
ybocs_cmp:Run	0.12	0.27	20	0.668	[-0.45, 0.69]

Right Caudate

Intercept	34.00	8.74	20	0.001	[15.77, 52.24]
Run	2.43	5.57	20	0.668	[-9.2, 14.05]
ybocs_cmp	0.12	0.63	20	0.849	[-1.19, 1.43]
ybocs_cmp:Run	-0.17	0.40	20	0.667	[-1.01, 0.66]

Right Hippocampus

Intercept	39.22	8.08	20	0.000	[22.37, 56.07]
Run	4.57	5.91	20	0.448	[-7.76, 16.9]
ybocs_cmp	-0.34	0.58	20	0.567	[-1.55, 0.87]
ybocs_cmp:Run	-0.33	0.42	20	0.448	[-1.22, 0.56]

Right Putamen

Intercept	52.88	10.16	20	0.000	[31.69, 74.08]
Run	0.43	8.79	20	0.962	[-17.91, 18.77]
ybocs_cmp	-0.11	0.73	20	0.885	[-1.63, 1.42]
ybocs_cmp:Run	0.09	0.63	20	0.882	[-1.22, 1.41]

Right Thalamus

Intercept	44.73	14.58	20	0.006	[14.32, 75.14]
Run	-1.80	8.03	20	0.825	[-18.55, 14.95]
ybocs_cmp	0.65	1.05	20	0.544	[-1.54, 2.83]

Table 6 (continued)

	ybocs_cmp:Run	0.04	0.58	20	0.942	[-1.16, 1.25]

Supplementary Motor Area

	Intercept	36.33	9.52	20	0.001	[16.47, 56.2]
	Run	-5.27	6.80	20	0.448	[-19.46, 8.93]
	ybocs_cmp	0.40	0.68	20	0.564	[-1.03, 1.83]
	ybocs_cmp:Run	0.27	0.49	20	0.590	[-0.75, 1.29]

Subcallosal Cortex

	Intercept	26.84	8.30	20	0.004	[9.53, 44.15]
	Run	1.20	4.36	20	0.787	[-7.9, 10.29]
	ybocs_cmp	0.10	0.60	20	0.868	[-1.14, 1.34]
	ybocs_cmp:Run	-0.12	0.31	20	0.714	[-0.77, 0.54]

Note. *$p_{uncorr} < .05$, **$p_{corr} < .05$.

Table 7 Y-BOCS Obsession Severity Sub-Score Effects On PWM Perfusion Across A Priori ROI

ROI	Variable	B/F	SE	df	p	95% CI
Central Opercular Cortex						
	Intercept	49.04	1.91	20	0.000	[45.05, 53.03]
	Run	-1.57	1.59	20	0.336	[-4.88, 1.75]
	ybocs_obs	-0.77	0.70	20	0.281	[-2.23, 0.68]
	ybocs_obs:Run	-0.33	0.58	20	0.576	[-1.54, 0.88]
Anterior Cingulate						
	Intercept	50.07	1.95	20	0.000	[46.01, 54.14]
	Run	-1.64	1.25	20	0.204	[-4.24, 0.96]
	ybocs_obs	-1.95	0.71	20	0.012*	[-3.44, -0.47]
	ybocs_obs:Run	0.05	0.45	20	0.919	[-0.9, 0.99]
Posterior Cingulate						
	Intercept	45.71	2.69	20	0.000	[40.1, 51.32]
	Run	-0.68	1.57	20	0.668	[-3.95, 2.59]
	ybocs_obs	0.08	0.98	20	0.940	[-1.97, 2.12]
	ybocs_obs:Run	-0.17	0.57	20	0.775	[-1.36, 1.03]
Frontal Medial Cortex						
	Intercept	32.74	2.36	19	0.000	[27.79, 37.68]
	Run	-0.39	2.07	19	0.851	[-4.73, 3.94]
	ybocs_obs	0.66	1.04	19	0.532	[-1.51, 2.83]
	ybocs_obs:Run	-0.59	0.91	19	0.525	[-2.49, 1.31]
Frontal Orbital Cortex						
	Intercept	35.06	1.86	20	0.000	[31.19, 38.93]
	Run	-0.72	1.76	20	0.688	[-4.38, 2.95]
	ybocs_obs	-0.97	0.68	20	0.168	[-2.38, 0.44]
	ybocs_obs:Run	-0.04	0.64	20	0.954	[-1.37, 1.3]
Insula						
	Intercept	39.09	1.25	20	0.000	[36.49, 41.69]
	Run	-0.81	1.26	20	0.528	[-3.43, 1.82]
	ybocs_obs	-0.88	0.45	20	0.068	[-1.83, 0.07]
	ybocs_obs:Run	0.05	0.46	20	0.908	[-0.9, 1.01]
Left Caudate						
	Intercept	35.03	2.12	20	0.000	[30.62, 39.45]
	Run	0.44	0.94	20	0.642	[-1.52, 2.41]
	ybocs_obs	-0.46	0.77	20	0.559	[-2.07, 1.15]
	ybocs_obs:Run	-0.21	0.34	20	0.548	[-0.93, 0.51]
Left Hippocampus						
	Intercept	34.99	1.40	20	0.000	[32.07, 37.92]
	Run	-1.23	1.33	20	0.367	[-4.01, 1.55]
	ybocs_obs	-0.72	0.51	20	0.174	[-1.79, 0.35]
	ybocs_obs:Run	-0.50	0.49	20	0.318	[-1.51, 0.52]
Left Putamen						
	Intercept	52.26	2.34	20	0.000	[47.37, 57.14]
	Run	1.75	1.51	20	0.260	[-1.39, 4.89]

Table 7 (continued)

	ybocs_obs	-1.61	0.85	20	0.074	[-3.39, 0.17]
	ybocs_obs:Run	-0.81	0.55	20	0.156	[-1.95, 0.34]
Left Thalamus						
	Intercept	55.50	3.37	20	0.000	[48.47, 62.52]
	Run	-2.38	1.86	20	0.216	[-6.25, 1.5]
	ybocs_obs	-0.34	1.23	20	0.783	[-2.9, 2.22]
	ybocs_obs:Run	-0.36	0.68	20	0.600	[-1.77, 1.05]
Paracingulate						
	Intercept	48.86	2.42	20	0.000	[43.81, 53.92]
	Run	-1.37	1.48	20	0.368	[-4.46, 1.73]
	ybocs_obs	-1.61	0.88	20	0.083	[-3.46, 0.23]
	ybocs_obs:Run	-0.13	0.54	20	0.819	[-1.25, 1]
Postcentral Gyrus						
	Intercept	43.62	2.45	19	0.000	[38.49, 48.76]
	Run	-0.36	1.16	19	0.759	[-2.79, 2.07]
	ybocs_obs	-1.97	1.08	19	0.083	[-4.22, 0.28]
	ybocs_obs:Run	0.44	0.51	19	0.399	[-0.63, 1.51]
Precentral Gyrus						
	Intercept	47.32	2.27	20	0.000	[42.59, 52.04]
	Run	-0.78	1.35	20	0.569	[-3.59, 2.03]
	ybocs_obs	-2.59	0.83	20	0.005*	[-4.31, -0.86]
	ybocs_obs:Run	-0.06	0.49	20	0.910	[-1.08, 0.97]
Precuneous						
	Intercept	41.89	2.08	20	0.000	[37.55, 46.23]
	Run	-0.35	0.81	20	0.667	[-2.05, 1.34]
	ybocs_obs	-1.77	0.76	20	0.03*	[-3.35, -0.19]
	ybocs_obs:Run	-0.06	0.30	20	0.840	[-0.68, 0.56]
Right Caudate						
	Intercept	35.65	1.76	20	0.000	[31.96, 39.33]
	Run	0.05	1.17	20	0.968	[-2.39, 2.49]
	ybocs_obs	-0.79	0.64	20	0.236	[-2.13, 0.56]
	ybocs_obs:Run	-0.43	0.43	20	0.327	[-1.32, 0.46]
Right Hippocampus						
	Intercept	34.62	1.53	20	0.000	[31.43, 37.82]
	Run	0.10	1.25	20	0.938	[-2.51, 2.71]
	ybocs_obs	-1.18	0.56	20	0.047*	[-2.34, -0.02]
	ybocs_obs:Run	-0.47	0.46	20	0.312	[-1.43, 0.48]
Right Putamen						
	Intercept	51.44	1.98	20	0.000	[47.31, 55.56]
	Run	1.71	1.87	20	0.370	[-2.19, 5.61]
	ybocs_obs	-1.28	0.72	20	0.091	[-2.79, 0.22]
	ybocs_obs:Run	-0.37	0.68	20	0.593	[-1.79, 1.05]
Right Thalamus						
	Intercept	53.52	3.14	20	0.000	[46.97, 60.08]
	Run	-1.22	1.64	20	0.467	[-4.64, 2.21]
	ybocs_obs	-0.38	1.15	20	0.741	[-2.77, 2.01]

Table 7 (continued)

	ybocs_obs:Run	0.83	0.60	20	0.179	[-0.42, 2.08]
Supplementary Motor Area						
	Intercept	41.78	1.82	20	0.000	[37.98, 45.59]
	Run	-1.63	1.41	20	0.261	[-4.56, 1.31]
	ybocs_obs	-1.91	0.66	20	0.009*	[-3.3, -0.52]
	ybocs_obs:Run	0.68	0.51	20	0.197	[-0.39, 1.75]
Subcallosal Cortex						
	Intercept	28.20	1.70	20	0.000	[24.66, 31.74]
	Run	-0.39	0.93	20	0.680	[-2.32, 1.55]
	ybocs_obs	-0.97	0.62	20	0.133	[-2.26, 0.32]
	ybocs_obs:Run	0.22	0.34	20	0.522	[-0.48, 0.93]

Note. *$p_{uncorr} < .05$, **$p_{corr} < .05$.

Table 8 Group (HC Vs. Low Obsession OCD) Effects On PWM Perfusion Across A Priori ROIs

ROI	Variable	B/F	SE	df	p	95% CI
Central Opercular Cortex						
	Intercept	44.86	2.01	32	0.000	[40.77, 48.96]
	Group	7.47	3.54	32	0.043*	[0.26, 14.67]
	Run	0.95	1.21	32	0.217	[-7.03, 1.66]
	Group:Run	-2.69	2.13	32	0.440	[-1.52, 3.42]
Anterior Cingulate						
	Intercept	46.51	1.85	32	0.000	[42.74, 50.27]
	Group	8.84	3.25	32	0.010*	[2.22, 15.46]
	Run	0.92	1.09	32	0.135	[-6.81, 0.96]
	Group:Run	-2.93	1.91	32	0.405	[-1.29, 3.13]
Posterior Cingulate						
	Intercept	45.28	2.51	32	0.000	[40.16, 50.4]
	Group	0.61	4.42	32	0.891	[-8.39, 9.61]
	Run	2.77	1.36	32	0.165	[-8.27, 1.47]
	Group:Run	-3.40	2.39	32	0.050	[0, 5.54]
Frontal Medial Cortex						
	Intercept	32.18	2.33	32	0.000	[27.43, 36.94]
	Group	3.80	4.10	32	0.362	[-4.56, 12.16]
	Run	2.01	1.70	32	0.233	[-9.72, 2.46]
	Group:Run	-3.63	2.99	32	0.246	[-1.46, 5.47]
Frontal Orbital Cortex						
	Intercept	33.40	1.70	32	0.000	[29.93, 36.88]
	Group	3.76	3.00	32	0.219	[-2.34, 9.86]
	Run	0.96	1.34	32	0.282	[-7.38, 2.22]
	Group:Run	-2.58	2.36	32	0.478	[-1.77, 3.69]
Insula						
	Intercept	36.19	1.54	32	0.000	[33.05, 39.32]
	Group	5.60	2.70	32	0.046*	[0.1, 11.11]
	Run	0.54	1.11	32	0.237	[-6.34, 1.63]
	Group:Run	-2.35	1.96	32	0.628	[-1.72, 2.81]
Left Caudate						
	Intercept	33.58	2.13	32	0.000	[29.23, 37.92]
	Group	1.91	3.75	32	0.615	[-5.74, 9.55]
	Run	0.17	0.69	32	0.499	[-1.64, 3.3]
	Group:Run	0.83	1.21	32	0.807	[-1.24, 1.58]
Left Hippocampus						
	Intercept	35.82	1.98	32	0.000	[31.79, 39.85]
	Group	1.37	3.48	32	0.695	[-5.71, 8.46]
	Run	2.04	1.15	32	0.134	[-7.21, 1.01]
	Group:Run	-3.10	2.02	32	0.085	[-0.3, 4.38]
Left Putamen						
	Intercept	51.75	2.86	32	0.000	[45.92, 57.57]
	Group	2.88	5.03	32	0.571	[-7.36, 13.12]

Table 8 (continued)

	Run	1.44	1.37	32	0.520	[-3.33, 6.46]
	Group:Run	1.56	2.40	32	0.301	[-1.35, 4.22]

Left Thalamus

	Intercept	56.19	3.78	32	0.000	[48.5, 63.88]
	Group	3.90	6.64	32	0.561	[-9.62, 17.42]
	Run	1.63	1.62	32	0.148	[-10.05, 1.58]
	Group:Run	-4.23	2.86	32	0.324	[-1.68, 4.94]

Paracingulate

	Intercept	44.73	2.30	32	0.000	[40.04, 49.42]
	Group	8.97	4.05	32	0.034*	[0.72, 17.22]
	Run	0.54	1.27	32	0.309	[-6.88, 2.25]
	Group:Run	-2.32	2.24	32	0.676	[-2.06, 3.13]

Postcentral Gyrus

	Intercept	36.19	2.47	32	0.000	[31.16, 41.22]
	Group	15.15	4.34	32	0.001**	[6.31, 24]
	Run	1.73	1.27	32	0.425	[-6.33, 2.73]
	Group:Run	-1.80	2.23	32	0.180	[-0.85, 4.31]

Precentral Gyrus

	Intercept	40.27	2.36	32	0.000	[35.46, 45.07]
	Group	14.25	4.15	32	0.002**	[5.8, 22.71]
	Run	2.38	1.30	32	0.210	[-7.58, 1.73]
	Group:Run	-2.93	2.29	32	0.076	[-0.27, 5.03]

Precuneous

	Intercept	37.81	2.20	32	0.000	[33.33, 42.3]
	Group	8.29	3.87	32	0.040*	[0.4, 16.18]
	Run	2.41	0.91	32	0.081	[-6.11, 0.38]
	Group:Run	-2.87	1.59	32	0.012*	[0.57, 4.26]

Right Caudate

	Intercept	33.64	2.05	32	0.000	[29.46, 37.81]
	Group	3.66	3.60	32	0.318	[-3.68, 10.99]
	Run	1.26	0.99	32	0.527	[-4.65, 2.43]
	Group:Run	-1.11	1.74	32	0.210	[-0.75, 3.28]

Right Hippocampus

	Intercept	36.20	1.76	32	0.000	[32.62, 39.79]
	Group	0.93	3.09	32	0.765	[-5.37, 7.24]
	Run	0.79	1.10	32	0.689	[-4.7, 3.14]
	Group:Run	-0.78	1.93	32	0.474	[-1.44, 3.02]

Right Putamen

	Intercept	50.18	2.38	32	0.000	[45.33, 55.04]
	Group	2.74	4.19	32	0.518	[-5.8, 11.27]
	Run	2.29	1.48	32	0.892	[-4.96, 5.67]
	Group:Run	0.36	2.61	32	0.134	[-0.74, 5.31]

Right Thalamus

	Intercept	54.50	3.43	32	0.000	[47.52, 61.48]
	Group	3.31	6.03	32	0.586	[-8.97, 15.59]
	Run	1.98	1.56	32	0.061	[-10.92, 0.27]

Table 8 (continued)

	Group:Run	-5.32	2.75	32	0.215	[-1.2, 5.16]
Supplementary Motor Area						
	Intercept	38.08	1.84	32	0.000	[34.33, 41.84]
	Group	8.29	3.24	32	0.015*	[1.69, 14.89]
	Run	1.17	1.43	32	0.123	[-9.08, 1.14]
	Group:Run	-3.97	2.51	32	0.420	[-1.74, 4.07]
Subcallosal Cortex						
	Intercept	33.28	2.06	32	0.000	[29.09, 37.47]
	Group	-3.09	3.62	32	0.400	[-10.45, 4.28]
	Run	2.54	0.88	31	0.008*	[-7.43, -1.22]
	Group:Run	-4.32	1.52	31	0.007*	[0.75, 4.33]

Note. *$p_{uncorr} < .05$, **$p_{corr} < .05$.

Table 9 Group (HC Vs. High Obsession OCD) Effects On PWM Perfusion Across A Priori ROIs

ROI	Variable	B/F	SE	df	p	95% CI
Central Opercular Cortex						
	Intercept	44.86	1.90	32	0.000	[40.99, 48.74]
	Group	0.88	3.34	32	0.793	[-5.92, 7.69]
	Run	0.95	1.14	32	0.409	[-1.36, 3.26]
	Group:Run	-2.35	2.00	32	0.248	[-6.42, 1.72]
Anterior Cingulate						
	Intercept	46.51	1.88	32	0.000	[42.68, 50.33]
	Group	-1.71	3.30	32	0.607	[-8.43, 5.01]
	Run	0.92	0.93	32	0.330	[-0.97, 2.8]
	Group:Run	-2.18	1.63	32	0.190	[-5.49, 1.13]
Posterior Cingulate						
	Intercept	45.28	2.28	32	0.000	[40.64, 49.92]
	Group	0.26	4.01	32	0.949	[-7.9, 8.42]
	Run	2.77	1.25	32	0.034*	[0.22, 5.32]
	Group:Run	-3.50	2.20	32	0.122	[-7.98, 0.98]
Frontal Medial Cortex						
	Intercept	32.18	2.45	32	0.000	[27.19, 37.17]
	Group	0.68	4.31	32	0.876	[-8.1, 9.45]
	Run	2.01	1.42	32	0.166	[-0.88, 4.9]
	Group:Run	-3.02	2.49	32	0.235	[-8.1, 2.06]
Frontal Orbital Cortex						
	Intercept	33.40	1.70	32	0.000	[29.94, 36.87]
	Group	-0.45	2.99	32	0.883	[-6.54, 5.65]
	Run	0.96	1.09	32	0.381	[-1.25, 3.17]
	Group:Run	-0.78	1.91	32	0.686	[-4.66, 3.11]
Insula						
	Intercept	36.19	1.55	32	0.000	[33.02, 39.35]
	Group	0.20	2.73	32	0.943	[-5.37, 5.76]
	Run	0.54	0.85	32	0.525	[-1.18, 2.27]
	Group:Run	-0.35	1.49	32	0.815	[-3.38, 2.68]
Left Caudate						
	Intercept	33.58	1.89	32	0.000	[29.72, 37.43]
	Group	1.01	3.33	32	0.764	[-5.77, 7.79]
	Run	0.17	0.82	32	0.836	[-1.5, 1.84]
	Group:Run	-0.28	1.44	32	0.846	[-3.21, 2.65]
Left Hippocampus						
	Intercept	35.82	1.90	32	0.000	[31.95, 39.68]
	Group	-3.02	3.33	32	0.371	[-9.81, 3.77]
	Run	2.04	1.26	32	0.116	[-0.53, 4.61]
	Group:Run	-3.44	2.22	32	0.131	[-7.96, 1.08]
Left Putamen						
	Intercept	51.75	2.60	32	0.000	[46.46, 57.04]
	Group	-1.86	4.56	32	0.686	[-11.16, 7.44]

Table 9 (continued)

	Run	1.44	1.02	32	0.170	[-0.65, 3.52]
	Group:Run	-0.94	1.80	32	0.605	[-4.6, 2.72]
Left Thalamus						
	Intercept	56.19	3.27	32	0.000	[49.53, 62.85]
	Group	-5.29	5.75	32	0.365	[-17, 6.42]
	Run	1.63	1.18	32	0.179	[-0.78, 4.04]
	Group:Run	-3.77	2.08	32	0.079	[-8.01, 0.47]
Paracingulate						
	Intercept	44.73	2.13	32	0.000	[40.38, 49.07]
	Group	-0.70	3.75	32	0.853	[-8.34, 6.94]
	Run	0.54	0.89	32	0.550	[-1.28, 2.36]
	Group:Run	-1.50	1.57	32	0.347	[-4.69, 1.7]
Postcentral Gyrus						
	Intercept	36.19	1.79	32	0.000	[32.54, 39.84]
	Group	1.34	3.15	32	0.673	[-5.08, 7.76]
	Run	1.73	1.12	32	0.132	[-0.55, 4.02]
	Group:Run	-0.96	1.97	32	0.629	[-4.98, 3.05]
Precentral Gyrus						
	Intercept	40.27	1.99	32	0.000	[36.22, 44.31]
	Group	-0.16	3.49	32	0.965	[-7.27, 6.96]
	Run	2.38	1.26	32	0.067	[-0.17, 4.94]
	Group:Run	-3.40	2.21	32	0.133	[-7.9, 1.1]
Precuneous						
	Intercept	37.81	1.92	32	0.000	[33.91, 41.72]
	Group	-0.14	3.37	32	0.968	[-7, 6.73]
	Run	2.41	0.83	32	0.007*	[0.72, 4.11]
	Group:Run	-2.67	1.46	32	0.077	[-5.65, 0.3]
Right Caudate						
	Intercept	33.64	1.97	32	0.000	[29.62, 37.65]
	Group	0.36	3.47	32	0.918	[-6.7, 7.42]
	Run	1.26	1.01	32	0.222	[-0.8, 3.33]
	Group:Run	-1.32	1.78	32	0.465	[-4.95, 2.31]
Right Hippocampus						
	Intercept	36.20	1.62	32	0.000	[32.89, 39.51]
	Group	-4.09	2.86	32	0.162	[-9.91, 1.73]
	Run	0.79	0.96	32	0.414	[-1.16, 2.75]
	Group:Run	-0.61	1.69	32	0.719	[-4.04, 2.82]
Right Putamen						
	Intercept	50.18	2.40	32	0.000	[45.29, 55.08]
	Group	-0.23	4.22	32	0.957	[-8.83, 8.37]
	Run	2.29	1.09	32	0.043*	[0.07, 4.5]
	Group:Run	-1.50	1.91	32	0.437	[-5.39, 2.39]
Right Thalamus						
	Intercept	54.50	2.97	32	0.000	[48.46, 60.54]
	Group	-5.27	5.21	32	0.320	[-15.89, 5.35]
	Run	1.98	1.26	32	0.126	[-0.59, 4.54]

Table 9 (continued)

	Group:Run	-1.07	2.21	32	0.633	[-5.58, 3.44]
Supplementary Motor Area						
	Intercept	38.08	1.75	32	0.000	[34.53, 41.64]
	Group	-0.89	3.07	32	0.775	[-7.14, 5.37]
	Run	1.17	1.22	32	0.345	[-1.31, 3.64]
	Group:Run	-1.61	2.14	32	0.456	[-5.97, 2.74]
Subcallosal Cortex						
	Intercept	33.28	2.15	32	0.000	[28.89, 37.66]
	Group	-7.07	3.79	32	0.071	[-14.78, 0.64]
	Run	2.54	0.94	31	0.011*	[0.61, 4.46]
	Group:Run	-1.53	1.63	31	0.357	[-4.86, 1.81]

Note. *p_{uncorr} < .05, **p_{corr} < .05.

Table 10 Group (Low Vs. High Obsession OCD) Effects On PWM Perfusion Across A Priori ROIs

ROI	Variable	B/F	SE	df	p	95% CI
Central Opercular Cortex						
	Intercept	58.91	5.90	20	0.000	[46.6, 71.22]
	Group	-6.58	3.73	20	0.093	[-14.37, 1.2]
	Run	-2.07	5.07	20	0.687	[-12.64, 8.49]
	Group:Run	0.34	3.20	20	0.917	[-6.35, 7.02]
Anterior Cingulate						
	Intercept	65.91	6.24	20	0.000	[52.88, 78.93]
	Group	-10.56	3.95	20	0.015*	[-18.79, -2.32]
	Run	-2.76	3.93	20	0.491	[-10.96, 5.44]
	Group:Run	0.75	2.49	20	0.767	[-4.44, 5.93]
Posterior Cingulate						
	Intercept	46.23	8.50	20	0.000	[28.5, 63.97]
	Group	-0.35	5.38	20	0.949	[-11.57, 10.87]
	Run	-0.53	4.96	20	0.916	[-10.89, 9.83]
	Group:Run	-0.10	3.14	20	0.974	[-6.65, 6.45]
Frontal Medial Cortex						
	Intercept	39.10	7.92	20	0.000	[22.57, 55.63]
	Group	-3.12	5.01	20	0.541	[-13.57, 7.33]
	Run	-2.24	6.64	20	0.740	[-16.09, 11.61]
	Group:Run	0.61	4.20	20	0.885	[-8.15, 9.38]
Frontal Orbital Cortex						
	Intercept	41.37	6.05	20	0.000	[28.74, 54]
	Group	-4.21	3.83	20	0.285	[-12.19, 3.78]
	Run	-3.42	5.52	20	0.542	[-14.93, 8.09]
	Group:Run	1.80	3.49	20	0.611	[-5.48, 9.08]
Insula						
	Intercept	47.20	3.97	20	0.000	[38.92, 55.47]
	Group	-5.40	2.51	20	0.044*	[-10.64, -0.17]
	Run	-3.81	3.92	20	0.342	[-11.99, 4.36]
	Group:Run	2.00	2.48	20	0.428	[-3.17, 7.17]
Left Caudate						
	Intercept	36.38	6.77	20	0.000	[22.27, 50.49]
	Group	-0.90	4.28	20	0.836	[-9.82, 8.03]
	Run	2.11	2.98	20	0.487	[-4.11, 8.33]
	Group:Run	-1.11	1.88	20	0.562	[-5.04, 2.82]
Left Hippocampus						
	Intercept	41.59	4.56	20	0.000	[32.07, 51.1]
	Group	-4.40	2.88	20	0.143	[-10.41, 1.62]
	Run	-0.72	4.32	20	0.869	[-9.74, 8.3]
	Group:Run	-0.34	2.73	20	0.902	[-6.04, 5.36]
Left Putamen						
	Intercept	59.37	8.13	20	0.000	[42.42, 76.32]

Table 10 (continued)

	Group	-4.74	5.14	20	0.367	[-15.46, 5.98]
	Run	5.50	4.93	20	0.278	[-4.79, 15.79]
	Group:Run	-2.50	3.12	20	0.432	[-9.01, 4.01]
Left Thalamus						
	Intercept	69.27	10.23	20	0.000	[47.94, 90.61]
	Group	-9.18	6.47	20	0.171	[-22.68, 4.31]
	Run	-3.07	5.91	20	0.610	[-15.4, 9.27]
	Group:Run	0.46	3.74	20	0.903	[-7.34, 8.26]
Paracingulate						
	Intercept	63.36	7.65	20	0.000	[47.4, 79.32]
	Group	-9.66	4.84	20	0.060	[-19.76, 0.43]
	Run	-2.60	4.69	20	0.586	[-12.38, 7.19]
	Group:Run	0.82	2.97	20	0.785	[-5.37, 7.01]
Postcentral Gyrus						
	Intercept	65.15	8.54	20	0.000	[47.34, 82.96]
	Group	-13.81	5.40	20	0.019*	[-25.07, -2.55]
	Run	-0.91	3.95	20	0.821	[-9.14, 7.33]
	Group:Run	0.84	2.50	20	0.740	[-4.37, 6.05]
Precentral Gyrus						
	Intercept	68.93	7.09	20	0.000	[54.13, 83.73]
	Group	-14.41	4.49	20	0.004*	[-23.77, -5.05]
	Run	-0.07	4.26	20	0.988	[-8.95, 8.81]
	Group:Run	-0.47	2.69	20	0.862	[-6.09, 5.14]
Precuneous						
	Intercept	54.53	6.84	20	0.000	[40.25, 68.81]
	Group	-8.43	4.33	20	0.066	[-17.46, 0.6]
	Run	-0.65	2.57	20	0.804	[-6.01, 4.72]
	Group:Run	0.19	1.63	20	0.906	[-3.2, 3.59]
Right Caudate						
	Intercept	40.59	5.80	20	0.000	[28.5, 52.69]
	Group	-3.30	3.67	20	0.379	[-10.95, 4.35]
	Run	0.36	3.79	20	0.925	[-7.55, 8.27]
	Group:Run	-0.21	2.40	20	0.931	[-5.21, 4.79]
Right Hippocampus						
	Intercept	42.16	5.30	20	0.000	[31.1, 53.22]
	Group	-5.02	3.35	20	0.150	[-12.02, 1.97]
	Run	-0.15	4.06	20	0.971	[-8.63, 8.32]
	Group:Run	0.17	2.57	20	0.949	[-5.19, 5.53]
Right Putamen						
	Intercept	55.89	6.73	20	0.000	[41.84, 69.94]
	Group	-2.97	4.26	20	0.494	[-11.85, 5.92]
	Run	4.50	5.92	20	0.456	[-7.85, 16.85]
	Group:Run	-1.86	3.74	20	0.625	[-9.67, 5.95]
Right Thalamus						

Table 10 (continued)

	Intercept	66.39	9.68	20	0.000	[46.21, 86.58]
	Group	-8.58	6.12	20	0.176	[-21.35, 4.19]
	Run	-7.60	5.23	20	0.161	[-18.51, 3.3]
	Group:Run	4.26	3.31	20	0.212	[-2.64, 11.15]
Supplementary Motor Area						
	Intercept	55.54	5.90	20	0.000	[43.24, 67.84]
	Group	-9.17	3.73	20	0.023*	[-16.95, -1.39]
	Run	-5.16	4.57	20	0.272	[-14.69, 4.36]
	Group:Run	2.36	2.89	20	0.424	[-3.67, 8.38]
Subcallosal Cortex						
	Intercept	34.18	5.52	20	0.000	[22.65, 45.7]
	Group	-3.98	3.49	20	0.268	[-11.27, 3.3]
	Run	-4.58	2.79	20	0.117	[-10.4, 1.25]
	Group:Run	2.79	1.77	20	0.130	[-0.89, 6.48]

Note. *$p_{uncorr} < .05$, **$p_{corr} < .05$.

Figure 1 Zero-Order Correlations Between Y-BOCS Obsession Scores and Perfusion Among A Priori ROIs
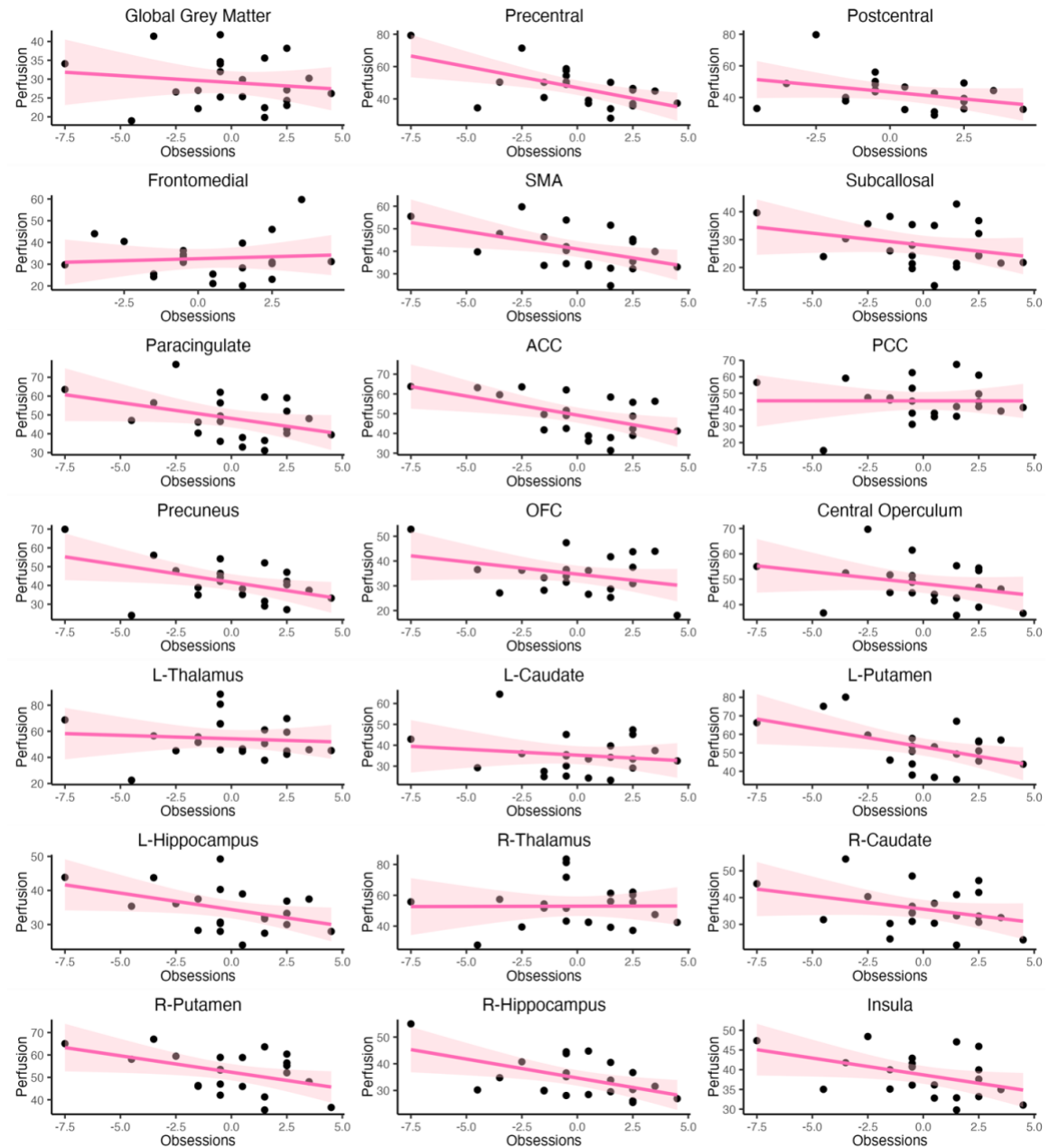
Note. Zero-order correlations between Y-BOCS obsession severity scores (centered, x-axis) and precision-weighted mean perfusion (y-axis) of global grey matter and a priori ROIs reveal consistent negative associations throughout the brain, though no correlations were significant with FDR correction.

Figure 2 OCD patients with lower severity obsessions demonstrate significantly higher PWM perfusion (y-axis) in the precentral and postcentral gyri relative to HCs.
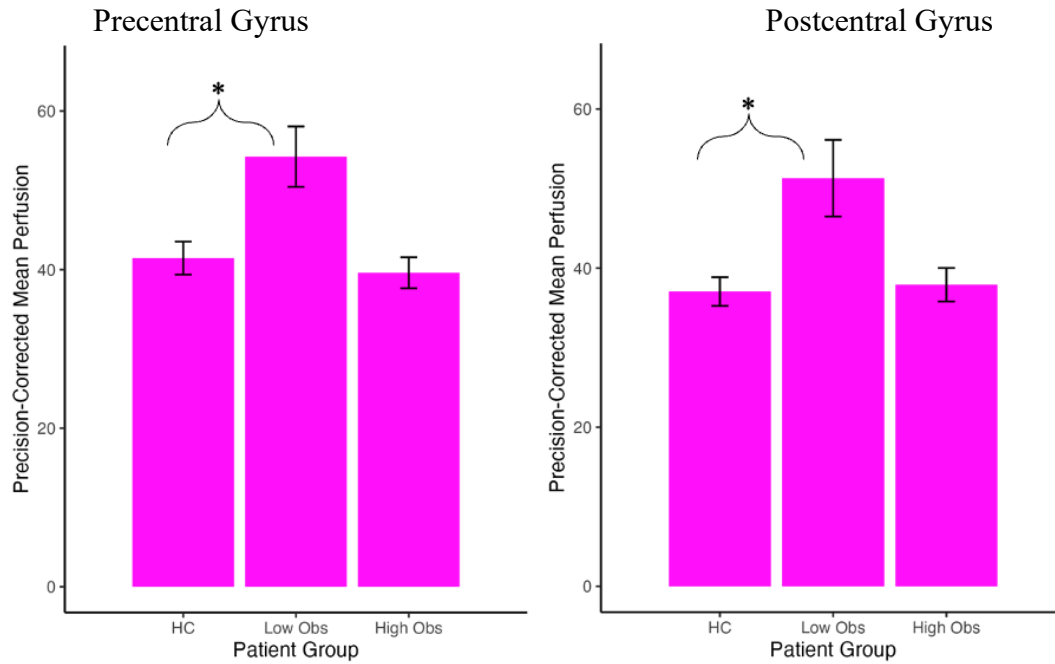
Note. Low Obsession OCD patients ("Low Obs") scored < 14 on the obsessional severity sub score, and High Obsession OCD patients ("High Obs") scored ≥ 14 on obsessional severity. Low Obsession OCD Patients demonstrate significantly higher perfusion than HCs in the pre- and post-central gyri after correcting for FDR.*p_{corr} < .05.

CHAPTER 4. DISCUSSION

This study aimed to characterize differences in rCBF between HCs and OCD patients using ASL. Based on prior rsFC and RCBF literature, and the two studies that used ASL perfusion abnormalities were expected in nodes of the CSTC and sensorimotor circuits in OCD patients, relative to HCs. Though most of the present study's findings did not survive FDR correction, many were trending towards significance in regions associated with the CSTC loop, CEN, DMN, SN, and sensorimotor network. Uncorrected main effects of Y-BOCS obsessional severity in the ACC, insula, precuneus, precentral gyrus, postcentral gyrus, SMA, and right hippocampus suggest that as obsessional severity increases, perfusion decreases in nodes of the CSTC loop, DMN, SN, and sensorimotor network. Post hoc probes separating OCD patients into high and low groups suggested that Low-Obsession OCD patients demonstrate higher DMN, SN, CSTC, and sensorimotor perfusion, relative to HCs and to High-Obsession OCD patients. However, the only group effects that survived FDR correction were between HCs and Low-Obsession OCD patients in the pre- and postcentral gyri, suggesting that OCD patients with low obsessions severity uniquely demonstrated higher perfusion in the sensorimotor network, compared to HCs.

The precentral gyrus, associated with controlling voluntary motor movement (Banker & Tadi, 2023), and the postcentral gyrus, associated with proprioception and sensory-memory formation (DiGuiseppi & Tadi, 2023), are both nodes of the sensorimotor network (Banker & Tadi, 2023; DiGuiseppi & Tadi, 2023). Prior theories of OCD pathophysiology describe abnormalities across and within three major circuits (Milad & Rauch, 2012). The sensorimotor-CSTC circuit, a more recent addition to

47

circuit-based models of OCD, plays a role in generating and controlling motor behaviors and incorporating sensory information (Bruin et al., 2023; Shephard et al., 2021; van den Heuvel et al., 2016). Specifically, altered sensorimotor-CSTC connectivity, or perfusion, could contribute to increased severity of perceptions that drive compulsions, as well as disruptions in inhibitory control over compulsions (Bruin et al., 2023; Shephard et al., 2021). In short, increased perfusion in the precentral and postcentral gyri among Low-Obsession OCD patients may indicate dysregulation in sensorimotor circuitry, leading to disrupted inhibition of automatic thoughts and/or behaviors (Bruin et al., 2023; Shephard et al., 2021).

The present study separated OCD patients into high and low obsessional severity, which is a notable departure from prior rCBF-OCD analytic choices. All prior rCBF OCD studies combined OCD patients with varying degrees of severity into a single group to identify group (HC v. OCD) effects on rCBF (Alptekin et al., 2001; Busatto et al., 2000; Diler et al., 2004; Guo et al., 2014; Harris et al., 1994; Karadağ et al., 2013; Lacerda et al., 2003; Lucey et al., 1995; Momosaka et al., 2020; Nakatani et al., 2003; Ota et al., 2020; Rubin et al., 1992). While all OCD patients analyzed meet a clinical cutoff for OCD, according to the respective diagnostic criteria used, unique neural abnormalities may underly differences between individuals with lower and higher symptom severity. Binning OCD patients into one group may suppress potential patient group differences. The present study suggests that, given the null main effects of Group between HCs and High-Obsession OCD patients, the inverse relationship between perfusion and obsession severity is likely driven by increased perfusion in Low-Obsession OCD patients.

The present study found null associations between Y-BOCS total and perfusion but significant effects using only the Y-BOS obsessions sub-score. Most rCBF-OCD studies, except for one (Lacerda et al., 2003), used only the Y-BOCS total score to explore associations between symptom severity and perfusion, rather than examining obsessions and compulsions sub-scores individually. Moreover, several studies found null associations between Y-BOCS total score and perfusion (Alptekin et al., 2001; Diler et al., 2004; Karadağ et al., 2013; Lacerda et al., 2003). While the Y-BOCS obsessions and Y-BOCS compulsions sub-scores often demonstrate a strong correlation with each other and the Y-BOCS total score (Goodman & Price, 1989), psychometric studies demonstrate that the obsessions and compulsions sub-scores are distinct (McKay et al., 1995), suggesting that OCD symptom severity (as measured by the Y-BOCS) may be better represented as, at least, two-dimensional (McKay et al., 1995). Moreover, future studies may benefit from keeping with the two-dimensional model of OCD, and use obsession and compulsion sub-scores, along with total scores, when exploring associations between OCD symptoms and regional perfusion.

Finding higher perfusion in sensorimotor nodes in OCD patients with less severe obsessions was surprising given the consistent evidence for sensorimotor hypoactivation and hypo-connectivity among OCD patients (Bruin et al., 2023), as well as the typically positive association between perfusion and resting state functional connectivity (rsFC) (Chen et al., 2015). Similar incongruencies between perfusion and rsFC have been reported in white matter (Aslan et al., 2011), but it is unclear why this phenomenon occurs. One possible theory is that relative to HCs, OCD patients demonstrating decreased sensorimotor-connectivity may exhibit increased sensorimotor-perfusion as a

compensatory mechanism, suggesting that sensorimotor circuits in OCD patients are perhaps less efficient, requiring more perfusion to maintain function (Aslan et al., 2011; Chai et al., 2018; Shephard et al., 2021). This theory would imply that OCD patients with more severe obsessions should demonstrate higher sensorimotor perfusion, relative to OCD patients with less severe obsessions, but the present study found the opposite trend.

Another potential explanation stems from a recently published rsFC study comparing OCD patients and HCs (Stern et al., 2022), in which perseverative thinking scores (Szkodny & Newman, 2019) were positively associated with DMN rsFC and negatively associated with sensorimotor rsFC (Stern et al., 2022). OCD patients who reported low perseverative thinking demonstrated the greatest discrepancy between sensorimotor and DMN rsFC, indicating sensorimotor network dominance (Stern et al., 2022). Additionally, sensorimotor dominance was positively associated with symmetry and incompleteness-related thoughts, but negatively associated with unacceptable thoughts (Stern et al., 2022). These findings suggest that OCD patients lower in perseverative thinking may engage in incompleteness-related obsessions more-so than unacceptable thoughts, underlying the observed heightened sensorimotor dominance (Stern et al., 2022). This reasoning may be relevant to why OCD patients with lower Y-BOCS obsession scores showed higher sensorimotor region perfusion compared to HCs in the present study. More specifically, sensorimotor regions may exert a diminished inhibitory influence on DMN regions as obsession severity increases, which leads to broader overall perfusion. Alternatively, considering that the Y-BOCS checklist scale does not evaluate incompleteness obsessions (Goodman & Price, 1989), individuals with lower obsession severity may simply engage in a more incompleteness-related obsessions, as opposed to

other obsession types, leading to higher sensorimotor perfusion. Future studies should explore associations between sensorimotor dominance, perfusion, obsession sub types, and obsessional severity to test these interpretations.

Alternatively, psychiatric symptoms may influence thought processes "at rest". For example, OCD patients, particularly those with severe obsessions, are more likely than HCs to obsess during resting state scans, which would recruit unique neural resources. Said otherwise, the "resting" state of highly obsessive OCD patients may not involve much rest. It is possible that highly obsessive OCD patients have higher sensorimotor perfusion relative to HCs at rest, but this effect may be suppressed by the recruitment of networks associated with obsessive thoughts, which are anticorrelated with sensorimotor and resting activation (Menon, 2011; Stern et al., 2022).

This idea of unique "resting" states among psychiatric patients sheds light on a larger issue in resting-state neuroimaging research: the conflation of task-independence with the absence of symptom manifestation. To circumvent this potential confound, future studies should measure the content of participants thoughts during resting-state scans to characterize more accurately the "resting" state of participants. Periodically asking participants the content of their thoughts during resting scans or even after scanning may provide a simple way to monitor the presence or absence of obsessions. Alternatively, investigators could include additional items on the resting state questionnaire (Delamillieure et al., 2010) to assess for obsessions. Additionally, associations between resting-states and perfusion could be tested experimentally by scanning before and after presentation of neutral vs. symptom provocative images.

CHAPTER 5. LIMITATIONS

The present study has several limitations worth noting. One of the most significant limitations is the use of pASL as a labeling scheme. pASL has an inferior SNR compared to cASL and pcASL for two reasons. Firstly, the labeling bolus duration for pASL is shorter (~1 second or less) than pcASL (Alsop et al., 2015). A shorter labeling duration yields a smaller bolus, which lowers the SNR (Alsop et al., 2015). Due to the utilization of pASL with a QUIPSS II modification in the current study, the bolus length is fixed, enhancing signal quantification (Wong et al., 1998b), but pcASL SNR still remains superior (Alsop et al., 2015). Secondly, pASL involves inverting the entire bolus at once with a single pulse at the base of the head, whereas cASL inverts blood as it passes through a labeling plane closer to the parenchyma (Alsop et al., 2015). The wider a distance labeled blood travels, the more signal may decay by the time labeled blood reaches brain regions, ultimately diminishing the SNR (Alsop et al., 2015; Wong et al., 1998a). Incorporating pASL in the current study potentially compromised image quality by introducing a lower SNR, thereby constraining the number of statistically significant effects that could withstand FDR correction.

Additionally, the present study's use of EPI as a readout approach is a significant limitation. EPI commonly results in signal loss produced by susceptibility-gradient inhomogeneity in areas adjacent to air-tissue interfaces, such as the OFC (Deichmann et al., 2003; Ota et al., 2020). Notably, neither the current study nor the two prior ASL-OCD studies demonstrated significant mPFC hyperperfusion in OCD patients (Momosaka et al., 2020; Ota et al., 2020). mCC hypoperfusion was reported by Momosaka and colleagues (2020), however. These null findings in anterior portions of the mPFC might

be related to both studies' use of echo planar imaging (EPI). Likewise, the use of EPI in the present study may have compromised the signal in anterior mPFC regions, contributing to null findings in areas frequently linked to OCD pathophysiology.

The present study had other methodological limitations including a smaller sample size use of ROI-based analyses, and use of the Harvard-Oxford Cortical and Subcortical Atlas. The present study's sample size was smaller than Momosaka (2020), but larger than Ota (2020). Because twenty a priori linear mixed-effects models were conducted in the present study, many results did not survive FDR correction. A larger sample would have been more representative and provided greater statistical power. Assessing rCBF using ROI-based analysis may improve power but compromise reproducibility and reliability (Ashburner & Friston, 2000; Harris & Pearlson, 1993; Momosaka et al., 2020). Additionally, if adjacent regions with distinct function are lumped together into larger ROI, their individual effects may be suppressed. For example, the Harvard-Oxford lumps the functionally distinct lOFC and mOFC (Milad & Rauch, 2007; Rauch et al., 1994, 2007) into one OFC category, potentially suppressing significant group effects in these regions. For these reasons, future OCD-perfusion studies should consider using voxel-based analyses in tandem with a more precisely parcellated atlas.

CHAPTER 6.   CONCLUSION

In conclusion, this study utilized pASL to characterize resting cerebral blood flow in individuals with OCD compared to HCs. Notably, individuals with lower obsessional severity demonstrated higher perfusion in the sensorimotor network, particularly in the precentral and postcentral gyri, indicating potential dysregulation in sensorimotor

circuitry. Future perfusion studies incorporating recommended methodology, larger

sample sizes, voxel-based analyses, and precise atlases are warranted to further explore

these observations and elucidate resting perfusion differences across OCD patients at

varying levels of severity. Last, studies should consider measuring whether patients are

truly resting during resting-state scans, using methods described above, to better

characterize resting-state differences between patients and HCs.

REFERENCES

Aguirre, G. K., Detre, J. A., & Wang, J. (2005). Perfusion fMRI for Functional Neuroimaging. International Review of Neurobiology, 66, 213–236. https://doi.org/10.1016/S0074-7742(05)66007-2

Alptekin, K., Degirmenci, B., Kivircik, B., Durak, H., Yemez, B., Derebek, E., & Tunca, Z. (2001). Tc-99m HMPAO brain perfusion SPECT in drug-free obsessive-compulsive patients without depression. Psychiatry Research: Neuroimaging, 107(1), 51–56. https://doi.org/10.1016/S0925-4927(01)00086-5

Alsop, D. C., Detre, J. A., Golay, X., Günther, M., Hendrikse, J., Hernandez-Garcia, L., Lu, H., MacIntosh, B. J., Parkes, L. M., Smits, M., van Osch, M. J. P., Wang, D. J. J., Wong, E. C., & Zaharchuk, G. (2015). Recommended implementation of arterial spin-labeled perfusion MRI for clinical applications: A consensus of the ISMRM perfusion study group and the European consortium for ASL in dementia. Magnetic Resonance in Medicine, 73(1), 102–116. https://doi.org/10.1002/mrm.25197

American Psychiatric Association. (2013). Obsessive-Compulsive and Related Disorders. In Diagnostic and statistical manual of mental disorders (5th ed.). https://doi.org/10.1176/appi.books.9780890425596.dsm06

An, S., Mataix-Cols, D., Lawrence, N., Wooderson, S., Giampietro, V., Speckens, A., Brammer, M., & Phillips, M. L. (2009). To discard or not to discard: The neural basis of hoarding symptoms in obsessive-compulsive disorder. Molecular Psychiatry, 14(3), 318–331.

Ashburner, J., & Friston, K. J. (2000). Voxel-based morphometry—The methods. NeuroImage, 11(6 Pt 1), 805–821. https://doi.org/10.1006/nimg.2000.0582

Aslan, S., Huang, H., Uh, J., Mishra, V., Xiao, G., van Osch, M. J. P., & Lu, H. (2011). White matter cerebral blood flow is inversely correlated with structural and functional connectivity in the human brain. NeuroImage, 56(3), 1145–1153. https://doi.org/10.1016/j.neuroimage.2011.02.082

Banca, P., Voon, V., Vestergaard, M. D., Philipiak, G., Almeida, I., Pocinho, F., Relvas, J., & Castelo-Branco, M. (2015). Imbalance in habitual versus goal directed neural systems during symptom provocation in obsessive-compulsive disorder. Brain, 138(3), 798–811. https://doi.org/10.1093/brain/awu379

Banker, L., & Tadi, P. (2023). Neuroanatomy, Precentral Gyrus. In StatPearls. StatPearls Publishing. http://www.ncbi.nlm.nih.gov/books/NBK544218/

Beucke, J. C., Sepulcre, J., Talukdar, T., Linnman, C., Zschenderlein, K., Endrass, T., Kaufmann, C., & Kathmann, N. (2013). Abnormally High Degree Connectivity of the Orbitofrontal Cortex in Obsessive-Compulsive Disorder. JAMA Psychiatry, 70(6), 619–629. https://doi.org/10.1001/jamapsychiatry.2013.173

Borogovac, A., & Asllani, I. (2012). Arterial spin labeling (ASL) fMRI: Advantages, theoretical constrains and experimental challenges in neurosciences. International Journal of Biomedical Imaging, 2012, 818456. https://doi.org/10.1155/2012/818456

Borogovac, A., Habeck, C., Small, S. A., & Asllani, I. (2010). Mapping brain function using a 30-day interval between baseline and activation: A novel arterial spin labeling fMRI approach. Journal of Cerebral Blood Flow and Metabolism, 30(10), 1721–1733. https://doi.org/10.1038/jcbfm.2010.89

Bruin, W. B., Abe, Y., Alonso, P., Anticevic, A., Backhausen, L. L., Balachander, S., Bargallo, N., Batistuzzo, M. C., Benedetti, F., Bertolin Triquell, S., Brem, S., Calesella, F., Couto, B., Denys, D. A. J. P., Echevarria, M. A. N., Eng, G. K., Ferreira, S., Feusner, J. D., Grazioplene, R. G., … van Wingen, G. A. (2023). The functional connectome in obsessive-compulsive disorder: Resting-state mega-analysis and machine learning classification for the ENIGMA-OCD consortium. Molecular Psychiatry, 1–13. https://doi.org/10.1038/s41380-023-02077-0

Bu, X., Hu, X., Zhang, L., Li, B., Zhou, M., Lu, L., Hu, X., Li, H., Yang, Y., Tang, W., Gong, Q., & Huang, X. (2019). Investigating the predictive value of different resting-state functional MRI parameters in obsessive-compulsive disorder. Translational Psychiatry, 9(1), 17. https://doi.org/10.1038/s41398-018-0362-9

Buchsbaum, M. S., Hollander, E., Pallanti, S., Rossi, N. B., Platholi, J., Newmark, R., Bloom, R., & Sood, E. (2006). Positron emission tomography imaging of risperidone augmentation in serotonin reuptake inhibitor-refractory patients. Neuropsychobiology, 53(3), 157–168. Scopus. https://doi.org/10.1159/000093342

Busatto, G. F., Zamignani, D. R., Buchpiguel, C. A., Garrido, G. E. J., Glabus, M. F., Rocha, E. T., Maia, A. F., Rosario-Campos, M. C., Campi Castro, C., Furuie, S. S., Gutierrez, M. A., McGuire, P. K., & Miguel, E. C. (2000). A voxel-based investigation of regional cerebral blood flow abnormalities in obsessive–compulsive disorder using single photon emission computed tomography (SPECT). Psychiatry Research: Neuroimaging, 99(1), 15–27. https://doi.org/10.1016/S0925-4927(00)00050-0

Bush, G., Luu, P., & Posner, M. I. (2000). Cognitive and emotional influences in anterior cingulate cortex. Trends in Cognitive Sciences, 4(6), 215–222. https://doi.org/10.1016/S1364-6613(00)01483-2

Carroll, T. J., Teneggi, V., Jobin, M., Squassante, L., Treyer, V., Hany, T. F., Burger, C., Wang, L., Bye, A., von Schulthess, G. K., & Buck, A. (2002). Absolute quantification of cerebral blood flow with magnetic resonance, reproducibility of the method, and comparison with H215O positron emission tomography. Journal of Cerebral Blood Flow & Metabolism, 22(9), 1149–1156. https://doi.org/10.1097/00004647-200209000-00013

Chai, W. J., Abd Hamid, A. I., & Abdullah, J. M. (2018). Working Memory From the Psychological and Neurosciences Perspectives: A Review. Frontiers in Psychology, 9. https://www.frontiersin.org/articles/10.3389/fpsyg.2018.00401

Chappell, M. A., Groves, A. R., MacIntosh, B. J., Donahue, M. J., Jezzard, P., & Woolrich, M. W. (2011). Partial volume correction of multiple inversion time arterial spin labeling MRI data. Magnetic Resonance in Medicine, 65(4), 1173–1183. https://doi.org/10.1002/mrm.22641

Chappell, M. A., Groves, A. R., Whitcher, B., & Woolrich, M. W. (2009). Variational Bayesian inference for a nonlinear forward model. IEEE Transactions on Signal Processing, 57(1), 223–236. https://doi.org/10.1109/TSP.2008.2005752

Chen, J. J., Jann, K., & Wang, D. J. J. (2015). Characterizing Resting-State Brain Function Using Arterial Spin Labeling. Brain Connectivity, 5(9), 527–542. https://doi.org/10.1089/brain.2015.0344

Christoff, K., Gordon, A. M., Smallwood, J., Smith, R., & Schooler, J. W. (2009). Experience sampling during fMRI reveals default network and executive system contributions to mind wandering. Proceedings of the National Academy of Sciences, 106(21), 8719–8724.

Deichmann, R., Gottfried, J. A., Hutton, C., & Turner, R. (2003). Optimized EPI for fMRI studies of the orbitofrontal cortex. NeuroImage, 19(2), 430–441. https://doi.org/10.1016/S1053-8119(03)00073-9

Delamillieure, P., Doucet, G., Mazoyer, B., Turbelin, M.-R., Delcroix, N., Mellet, E., Zago, L., Crivello, F., Petit, L., Tzourio-Mazoyer, N., & Joliot, M. (2010). The resting state questionnaire: An introspective questionnaire for evaluation of inner experience during the conscious resting state. Brain Research Bulletin, 81(6), 565–573. https://doi.org/10.1016/j.brainresbull.2009.11.014

Desikan, R. S., Ségonne, F., Fischl, B., Quinn, B. T., Dickerson, B. C., Blacker, D., Buckner, R. L., Dale, A. M., Maguire, R. P., Hyman, B. T., & others. (2006). An automated labeling system for subdividing the human cerebral cortex on MRI scans into gyral based regions of interest. Neuroimage, 31(3), 968–980.

Detre, J. A., & Wang, J. (2002). Technical aspects and utility of fMRI using BOLD and ASL. Clinical Neurophysiology, 113(5), 621–634. https://doi.org/10.1016/S1388-2457(02)00038-X

DiGuiseppi, J., & Tadi, P. (2023). Neuroanatomy, Postcentral Gyrus. In StatPearls. StatPearls Publishing. http://www.ncbi.nlm.nih.gov/books/NBK549825/

Diler, R. S., Kibar, M., & Avci, A. (2004). Pharmacotherapy and regional cerebral blood flow in children with obsessive compulsive disorder. Yonsei Medical Journal, 45(1), 90–99. https://doi.org/10.3349/ymj.2004.45.1.90

Duhamel, G., De Bazelaire, C., & Alsop, D. C. (2003). Evaluation of systematic quantification errors in velocity-selective arterial spin labeling of the brain.

Magnetic Resonance in Medicine, 50(1), 145–153.
https://doi.org/10.1002/mrm.10510

Etkin, A., Egner, T., & Kalisch, R. (2011). Emotional processing in anterior cingulate and medial prefrontal cortex. Trends in Cognitive Sciences, 15(2), 85–93. https://doi.org/10.1016/j.tics.2010.11.004

Fan, A. P., Jahanian, H., Holdsworth, S. J., & Zaharchuk, G. (2016). Comparison of cerebral blood flow measurement with [15O]-water positron emission tomography and arterial spin labeling magnetic resonance imaging: A systematic review. Journal of Cerebral Blood Flow & Metabolism, 36(5), 842–861. https://doi.org/10.1177/0271678X16636393

Fan, J., Zhong, M., Gan, J., Liu, W., Niu, C., Liao, H., Zhang, H., Tan, C., Yi, J., & Zhu, X. (2017). Spontaneous neural activity in the right superior temporal gyrus and left middle temporal gyrus is associated with insight level in obsessive-compulsive disorder. Journal of Affective Disorders, 207, 203–211. https://doi.org/10.1016/j.jad.2016.08.027

Floyd, T. F., Maldjian, J., Gonzales-Atavales, J., Alsop, D., & Detre, J. (2001). Test-retest stability with continuous arterial spin labeled (CASL) perfusion MRI in regional measurement of cerebral blood flow. Proc Intl Soc Magn Reson Med, 9, 1569.

Foa, E. B., Kozak, M. J., Goodman, W. K., Hollander, E., & et al. (1995). "DSM-IV field trial: Obsessive-compulsive disorder": Correction. The American Journal of Psychiatry, 152(4), 654–654. https://doi.org/10.1176/ajp.152.4.654-a

Fox, K. C., Spreng, R. N., Ellamil, M., Andrews-Hanna, J. R., & Christoff, K. (2015). The wandering brain: Meta-analysis of functional neuroimaging studies of mind-wandering and related spontaneous thought processes. Neuroimage, 111, 611–621.

Fox, M. D., & Raichle, M. E. (2007). Spontaneous fluctuations in brain activity observed with functional magnetic resonance imaging. Nature Reviews Neuroscience, 8(9), 700–711.

Frazier, J. A., Chiu, S., Breeze, J. L., Makris, N., Lange, N., Kennedy, D. N., Herbert, M. R., Bent, E. K., Koneru, V. K., Dieterich, M. E., & others. (2005). Structural brain magnetic resonance imaging of limbic and thalamic volumes in pediatric bipolar disorder. American Journal of Psychiatry, 162(7), 1256–1265.

Fullana, M. A., Mataix-Cols, D., Caspi, A., Harrington, H., Grisham, J. R., Moffitt, T. E., & Poulton, R. (2009). Obsessions and compulsions in the community: Prevalence, interference, help-seeking, developmental stability, and co-occurring psychiatric conditions. American Journal of Psychiatry, 166(3), 329–336. https://doi.org/10.1176/appi.ajp.2008.08071006

Goldstein, J. M., Seidman, L. J., Makris, N., Ahern, T., O'Brien, L. M., Caviness Jr, V. S., Kennedy, D. N., Faraone, S. V., & Tsuang, M. T. (2007). Hypothalamic

abnormalities in schizophrenia: Sex effects and genetic vulnerability. Biological Psychiatry, 61(8), 935–945.

Goodman, W. K., & Price, L. H. (1989). The Yale-Brown obsessive compulsive scale: I. Development, use, and reliability. Arch Gen Psychiatry, 46(11).

Goodman, W. K., Price, L. H., Rasmussen, S. A., & Mazure, C. (1989). The Yale-Brown Obsessive Compulsive Scale: II. Validity. Archives of General Psychiatry, 46(11), 1012–1016. https://doi.org/10.1001/archpsyc.1989.01810110054008

Goodman, W. K., Price, L. H., Rasmussen, S. A., Mazure, C., Fleischmann, R. L., Hill, C. L., Heninger, G. R., & Charney, D. S. (1989). The Yale-Brown obsessive compulsive scale: I. Development, use, and reliability. Archives of General Psychiatry, 46(11), 1006–1011.

Graybiel, A. M., & Rauch, S. L. (2000). Toward a neurobiology of obsessive-compulsive disorder. Neuron, 28(2), 343–347. https://doi.org/10.1016/S0896-6273(00)00113-6

Guo, H., Zhao, N., Li, Z., Zhu, B., Cui, H., & Li, Y. (2014). Regional cerebral blood flow and cognitive function in patients with obsessive-compulsive disorder. Arquivos de Neuro-Psiquiatria, 72, 44–48.

Gürsel, D. A., Avram, M., Sorg, C., Brandl, F., & Koch, K. (2018). Frontoparietal areas link impairments of large-scale intrinsic brain networks with aberrant fronto-striatal interactions in OCD: A meta-analysis of resting-state functional connectivity. Neuroscience & Biobehavioral Reviews, 87, 151–160. https://doi.org/10.1016/j.neubiorev.2018.01.016

Hamilton, M. (1960). A rating scale for depression. Journal of Neurology, Neurosurgery, and Psychiatry, 23(1), 56.

Hansen, E. S., Hasselbalch, S., Law, I., & Bolwig, T. G. (2002). The caudate nucleus in obsessive—Compulsive disorder. Reduced metabolism following treatment with paroxetine: A PET study. International Journal of Neuropsychopharmacology, 5(1), 1–10.

Harris, G. J., Hoehn-Saric, R., Lewis, R., Pearlson, G. D., & Streeter, C. (1994). Mapping of SPECT regional cerebral perfusion abnormalities in obsessive-compulsive disorder. Human Brain Mapping, 1(4), 237–248. https://doi.org/10.1002/hbm.460010403

Harris, G. J., & Pearlson, G. D. (1993). MRI-guided region of interest placement on emission computed tomograms. Psychiatry Research: Neuroimaging, 50(1), 57–63. https://doi.org/10.1016/0925-4927(93)90024-C

Hendler, T., Goshen, E., Zwas, S. T., Sasson, Y., Gal, G., & Zohar, J. (2003). Brain reactivity to specific symptom provocation indicates prospective therapeutic outcome in OCD. Psychiatry Research: Neuroimaging, 124(2), 87–103.

Hoogenraad, F. G. C., Pouwels, P. J. W., Hofman, M. B. M., Reichenbach, J. R., Sprenger, M., & Haacke, E. M. (2001). Quantitative differentiation between

BOLD models in fMRI. Magnetic Resonance in Medicine, 45(2), 233–246. https://doi.org/10.1002/1522-2594(200102)45:2<233::AID-MRM1032>3.0.CO;2-W

Hou, J., Wu, W., Lin, Y., Wang, J., Zhou, D., Guo, J., Gu, S., He, M., Ahmed, S., Hu, J., Qu, W., & Li, H. (2012). Localization of cerebral functional deficits in patients with obsessive-compulsive disorder: A resting-state fMRI study. Journal of Affective Disorders, 138(3), 313–321. https://doi.org/10.1016/j.jad.2012.01.022

Karadağ, F., Kalkan Oğuzhanoğlu, N., Yüksel, D., Kıraç, S., Cura, C., Ozdel, O., & Ateşci, F. (2013). The comparison of pre- and post-treatment (99m)Tc HMPAO brain SPECT images in patients with obsessive-compulsive disorder. Psychiatry Research, 213(2), 169–177. https://doi.org/10.1016/j.pscychresns.2012.07.005

Kessler, R. C., Chiu, W. T., Demler, O., & Walters, E. E. (2005). Prevalence, severity, and comorbidity of 12-month DSM-IV disorders in the National Comorbidity Survey Replicatio. Archives of General Psychiatry, 62(6), 617–627. https://doi.org/10.1001/archpsyc.62.6.617

Koran, L. M., Thienemann, M. L., & Davenport, R. (1996). Quality of life for patients with obsessive-compulsive disorder. The American Journal of Psychiatry, 153(6), 783–788. https://doi.org/10.1176/ajp.153.6.783

Kucyi, A., Esterman, M., Riley, C. S., & Valera, E. M. (2016). Spontaneous default network activity reflects behavioral variability independent of mind-wandering. Proceedings of the National Academy of Sciences, 113(48), 13899–13904. https://doi.org/10.1073/pnas.1611743113

Lacerda, A. L. T., Dalgalarrondo, P., Caetano, D., Camargo, E. E., Etchebehere, E. C. S. C., & Soares, J. C. (2003). Elevated thalamic and prefrontal regional cerebral blood flow in obsessive-compulsive disorder: A SPECT study. Psychiatry Research, 123(2), 125–134. https://doi.org/10.1016/s0925-4927(03)00061-1

Li, F., Lui, S., Huang, X. Q., Wu, Q., Li, B., Yang, Y., & Gong, Q. (2011, March 3). Localization of cerebral functional deficits in drug-naive obsessive-compulsive disorder using resting-state fMRI [Text]. ECR 2011 EPOS; European Congress of Radiology - ECR 2011. https://epos.myesr.org/poster/esr/ecr2011/C-0161

Liu, J., Bu, X., Hu, X., Li, H., Cao, L., Gao, Y., Liang, K., Zhang, L., Lu, L., Hu, X., Wang, Y., Gong, Q., & Huang, X. (2021). Temporal variability of regional intrinsic neural activity in drug-naïve patients with obsessive-compulsive disorder. Human Brain Mapping, 42(12), 3792–3803. https://doi.org/10.1002/hbm.25465

Liu, T. (2015). Perfusion imaging with arterial spin labeling MRI. Brain Mapping, 149–154. https://doi.org/10.1016/B978-0-12-397025-1.00017-8

Long, J., Luo, L., Guo, Y., You, W., Li, Q., Li, B., Tang, W., Yang, Y., Kemp, G. J., Sweeney, J. A., Li, F., & Gong, Q. (2021). Altered spontaneous activity and effective connectivity of the anterior cingulate cortex in obsessive-compulsive

disorder. The Journal of Comparative Neurology, 529(2), 296–310. https://doi.org/10.1002/cne.24948

Lucey, J. V., Costa, D. C., Blanes, T., Busatto, G. F., Pilowsky, L. S., Takei, N., Marks, I. M., Ell, P. J., & Kerwin, R. W. (1995). Regional cerebral blood flow in obsessive-compulsive disordered patients at rest: Differential correlates with obsessive–compulsive and anxious–avoidant dimensions. The British Journal of Psychiatry, 167(5), 629–634. https://doi.org/10.1192/bjp.167.5.629

Ma, J.-D., Wang, C.-H., Huang, P., Wang, X., Shi, L.-J., Li, H.-F., Sang, D.-E., Kou, S.-J., Li, Z.-R., Zhao, H.-Z., Lian, H.-K., & Hu, X.-Z. (2021). Effects of short-term cognitive-coping therapy on resting-state brain function in obsessive-compulsive disorder. Brain and Behavior, 11(4), e02059. https://doi.org/10.1002/brb3.2059

Ma, Y., Zhao, Q., Xu, T., Wang, P., Gu, Q., & Wang, Z. (2021). Resting state functional brain imaging in obsessive-compulsive disorder across genders. World Journal of Biological Psychiatry. Scopus. https://doi.org/10.1080/15622975.2021.1938669

Makris, N., Goldstein, J. M., Kennedy, D., Hodge, S. M., Caviness, V. S., Faraone, S. V., Tsuang, M. T., & Seidman, L. J. (2006). Decreased volume of left and total anterior insular lobule in schizophrenia. Schizophrenia Research, 83(2–3), 155–171.

Mason, M. F., Norton, M. I., Van Horn, J. D., Wegner, D. M., Grafton, S. T., & Macrae, C. N. (2007). Wandering minds: The default network and stimulus-independent thought. Science, 315(5810), 393–395.

McKay, D., Danyko, S., Neziroglu, F., & Yaryura-Tobias, J. A. (1995). Factor structure of the Yale-Brown Obsessive-Compulsive Scale: A two dimensional measure. Behaviour Research and Therapy, 33(7), 865–869.

Menon, V. (2011). Large-scale brain networks and psychopathology: A unifying triple network model. Trends in Cognitive Sciences, 15(10), 483–506. https://doi.org/10.1016/j.tics.2011.08.003

Milad, M. R., & Rauch, S. L. (2007). The role of the orbitofrontal cortex in anxiety disorders. Annals of the New York Academy of Sciences, 1121(1), 546–561.

Milad, M. R., & Rauch, S. L. (2012). Obsessive-compulsive disorder: Beyond segregated cortico-striatal pathways. Trends in Cognitive Sciences, 16(1), 43–51. https://doi.org/10.1016/j.tics.2011.11.003

Momosaka, D., Togao, O., Hiwatashi, A., Yamashita, K., Kikuchi, K., Tomiyama, H., Nakao, T., Murayama, K., Suzuki, Y., & Honda, H. (2020). A voxel-based analysis of cerebral blood flow abnormalities in obsessive-compulsive disorder using pseudo-continuous arterial spin labeling MRI. PLOS ONE, 15(7), e0236512. https://doi.org/10.1371/journal.pone.0236512

Nakatani, E., Nakgawa, A., Ohara, Y., Goto, S., Uozumi, N., Iwakiri, M., Yamamoto, Y., Motomura, K., Iikura, Y., & Yamagami, T. (2003). Effects of behavior therapy on regional cerebral blood flow in obsessive–compulsive disorder. Psychiatry

Research: Neuroimaging, 124(2), 113–120. https://doi.org/10.1016/S0925-4927(03)00069-6

Norris, D. G., & Schwarzbauer, C. (1999). Velocity selective radiofrequency pulse trains. Journal of Magnetic Resonance, 137(1), 231–236.

Ota, M., Kanie, A., Kobayashi, Y., Nakajima, A., Sato, N., & Horikoshi, M. (2020). Pseudo-continuous arterial spin labeling MRI study of patients with obsessive–compulsive disorder. Psychiatry Research: Neuroimaging, 303, 111124. https://doi.org/10.1016/j.pscychresns.2020.111124

Parkes, L. M., Rashid, W., Chard, D. T., & Tofts, P. S. (2004). Normal cerebral perfusion measurements using arterial spin labeling: Reproducibility, stability, and age and gender effects. Magnetic Resonance in Medicine: An Official Journal of the International Society for Magnetic Resonance in Medicine, 51(4), 736–743.

Perani, D., Colombo, C., Bressi, S., Bonfanti, A., Grassi, F., Scarone, S., Bellodi, L., Smeraldi, E., & Fazio, F. (1995). [18F] FDG PET study in obsessive–compulsive disorder: A clinical/metabolic correlation study after treatment. The British Journal of Psychiatry, 166(2), 244–250.

Rauch, S. L., Jenike, M. A., Alpert, N. M., Baer, L., Breiter, H. C., Savage, C. R., & Fischman, A. J. (1994). Regional cerebral blood flow measured during symptom provocation in obsessive-compulsive disorder using oxygen 15-labeled carbon dioxide and positron emission tomography. Archives of General Psychiatry, 51(1), 62–70. https://doi.org/10.1001/archpsyc.1994.03950010062008

Rauch, S. L., Wedig, M. M., Wright, C. I., Martis, B., McMullin, K. G., Shin, L. M., Cannistraro, P. A., & Wilhelm, S. (2007). Functional magnetic resonance imaging study of regional brain activation during implicit sequence learning in obsessive–compulsive disorder. Biological Psychiatry, 61(3), 330–336.

Ravizza, L., Maina, G., & Bogetto, F. (1997). Episodic and chronic obsessive-compulsive disorder. Depression and Anxiety, 6(4), 154–158. https://doi.org/10.1002/(SICI)1520-6394(1997)6:4<154::AID-DA4>3.0.CO;2-C

Rubin, R. T., Villanueva-Meyer, J., Ananth, J., Trajmar, P. G., & Mena, I. (1992). Regional xenon 133 cerebral blood flow and cerebral technetium 99m HMPAO uptake in unmedicated patients with obsessive-compulsive disorder and matched normal control subjects: Determination by high-resolution single-photon emission computed tomography. Archives of General Psychiatry, 49(9), 695–702. https://doi.org/10.1001/archpsyc.1992.01820090023004

Ruscio, A. M., Stein, D. J., Chiu, W. T., & Kessler, R. C. (2010). The epidemiology of obsessive-compulsive disorder in the National Comorbidity Survey Replication. Molecular Psychiatry, 15(1), 53–63. https://doi.org/10.1038/mp.2008.94

Saxena, S., O'Neill, J., & Rauch, S. L. (2009). The role of cingulate cortex dysfunction in obsessive-compulsive disorder (B. Vogt, Ed.; Vol. 1, pp. 588–606). Oxford University Press.

Shephard, E., Stern, E. R., van den Heuvel, O. A., Costa, D. L. C., Batistuzzo, M. C., Godoy, P. B. G., Lopes, A. C., Brunoni, A. R., Hoexter, M. Q., Shavitt, R. G., Reddy, J. Y. C., Lochner, C., Stein, D. J., Simpson, H. B., & Miguel, E. C. (2021). Toward a neurocircuit-based taxonomy to guide treatment of obsessive-compulsive disorder. Molecular Psychiatry, 26(9), 4583–4604. https://doi.org/10.1038/s41380-020-01007-8

Shulman, R. G., Rothman, D. L., & Hyder, F. (2007). A BOLD search for baseline. NeuroImage, 36(2), 277–281. https://doi.org/10.1016/j.neuroimage.2006.11.035

Stern, E. R., Eng, G. K., De Nadai, A. S., Iosifescu, D. V., Tobe, R. H., & Collins, K. A. (2022). Imbalance between default mode and sensorimotor connectivity is associated with perseverative thinking in obsessive-compulsive disorder. Translational Psychiatry, 12(1), Article 1. https://doi.org/10.1038/s41398-022-01780-w

Swedo, S. E., Rapoport, J. L., Leonard, H., Lenane, M., & Cheslow, D. (1989). Obsessive-compulsive disorder in children and adolescents: Clinical phenomenology of 70 consecutive cases. Archives of General Psychiatry, 46(4), 335–341.

Szkodny, L. E., & Newman, M. G. (2019). Delineating characteristics of maladaptive repetitive thought: Development and preliminary validation of the Perseverative Cognitions Questionnaire. Assessment, 26(6), 1084–1104.

van den Heuvel, O. A., van Wingen, G., Soriano-Mas, C., Alonso, P., Chamberlain, S. R., Nakamae, T., Denys, D., Goudriaan, A. E., & Veltman, D. J. (2016). Brain circuitry of compulsivity. European Neuropsychopharmacology, 26(5), 810–827. https://doi.org/10.1016/j.euroneuro.2015.12.005

Wang, J., Aguirre, G. K., Kimberg, D. Y., Roc, A. C., Li, L., & Detre, J. A. (2003). Arterial spin labeling perfusion fMRI with very low task frequency. Magnetic Resonance in Medicine, 49(5), 796–802. https://doi.org/10.1002/mrm.10437

Wintermark, M., Sesay, M., Barbier, E., Borbély, K., Dillon, W. P., Eastwood, J. D., Glenn, T. C., Grandin, C. B., Pedraza, S., Soustiel, J.-F., Nariai, T., Zaharchuk, G., Caillé, J.-M., Dousset, V., & Yonas, H. (2005). Comparative overview of brain perfusion imaging techniques. Stroke, 36(9), e83–e99. https://doi.org/10.1161/01.STR.0000177884.72657.8b

Wolff, S. D., & Balaban, R. S. (1989). Magnetization transfer contrast (MTC) and tissue water proton relaxation in vivo. Magnetic Resonance in Medicine, 10(1), 135–144. https://doi.org/10.1002/mrm.1910100113

Wong, E. C., Buxton, R. B., & Frank, L. R. (1998a). A theoretical and experimental comparison of continuous and pulsed arterial spin labeling techniques for quantitative perfusion imaging. Magnetic Resonance in Medicine, 40(3), 348–355. https://doi.org/10.1002/mrm.1910400303

Wong, E. C., Buxton, R. B., & Frank, L. R. (1998b). Quantitative imaging of perfusion using a single subtraction (QUIPSS and QUIPSS II). Magnetic Resonance in Medicine, 39(5), 702–708. https://doi.org/10.1002/mrm.1910390506

Xia, J., Fan, J., Du, H., Liu, W., Li, S., Zhu, J., Yi, J., Tan, C., & Zhu, X. (2019). Abnormal spontaneous neural activity in the medial prefrontal cortex and right superior temporal gyrus correlates with anhedonia severity in obsessive-compulsive disorder. Journal of Affective Disorders, 259, 47–55. https://doi.org/10.1016/j.jad.2019.08.019

Xia, J., Fan, J., Liu, W., Du, H., Zhu, J., Yi, J., Tan, C., & Zhu, X. (2020). Functional connectivity within the salience network differentiates autogenous- from reactive-type obsessive-compulsive disorder. Progress in Neuro-Psychopharmacology & Biological Psychiatry, 98, 109813. https://doi.org/10.1016/j.pnpbp.2019.109813

Yang, X., Hu, X., Tang, W., Li, B., Yang, Y., Gong, Q., & Huang, X. (2019). Intrinsic brain abnormalities in drug-naive patients with obsessive-compulsive disorder: A resting-state functional MRI study. Journal of Affective Disorders, 245, 861–868. https://doi.org/10.1016/j.jad.2018.11.080

Zaharchuk, G., Ledden, P. J., Kwong, K. K., Reese, T. G., Rosen, B. R., & Wald, L. L. (1999). Multislice perfusion and perfusion territory imaging in humans with separate label and image coils. Magnetic Resonance in Medicine: An Official Journal of the International Society for Magnetic Resonance in Medicine, 41(6), 1093–1098.

Zang, Yong, H., Chao-Zhe, Z., Qing-Jiu, C., Man-Qiu, S., Meng, L., Li-Xia, T., Tian-Zi, J., & Yu-Feng, W. (2007). Altered baseline brain activity in children with ADHD revealed by resting-state functional MRI. Brain and Development, 29(2), 83–91. https://doi.org/10.1016/j.braindev.2006.07.002

Zhang, Y., Liao, J., Li, Q., Zhang, X., Liu, L., Yan, J., Zhang, D., Yan, H., & Yue, W. (2021). Altered resting-state brain activity in schizophrenia and obsessive-compulsive disorder compared with non-psychiatric controls: Commonalities and distinctions across disorders. Frontiers in Psychiatry, 12, 681701. https://doi.org/10.3389/fpsyt.2021.681701

Zhao, H.-Z., Wang, C.-H., Gao, Z.-Z., Ma, J.-D., Huang, P., Li, H.-F., Sang, D.-E., Shan, X.-W., Kou, S.-J., Li, Z.-R., Ma, L., Zhang, Z.-H., Zhang, J.-H., Ouyang, H., Lian, H.-K., Zang, Y.-F., & Hu, X.-Z. (2017). Effectiveness of cognitive-coping therapy and alteration of resting-state brain function in obsessive-compulsive disorder. Journal of Affective Disorders, 208, 184–190. https://doi.org/10.1016/j.jad.2016.10.015

Zhou, X., & Lei, X. (2018). Wandering Minds with Wandering Brain Networks. Neuroscience Bulletin, 34(6), 1017–1028. https://doi.org/10.1007/s12264-018-0278-7

Zhu, Y., Fan, Q., Zhang, H., Qiu, J., Tan, L., Xiao, Z., Tong, S., Chen, J., & Li, Y. (2016). Altered intrinsic insular activity predicts symptom severity in unmedicated obsessive-compulsive disorder patients: A resting state functional magnetic resonance imaging study. BMC Psychiatry, 16(1), 104. https://doi.org/10.1186/s12888-016-0806-9

Zhu, Y., Fan, Q., Zhang, Z., Zhang, H., Tong, S., & Li, Y. (2015). Spontaneous neuronal activity in insula predicts symptom severity of unmedicated obsessive compulsive disorder adults. Proceedings of the Annual International Conference of the IEEE Engineering in Medicine and Biology Society, EMBS, 2015-November, 5445–5448. Scopus. https://doi.org/10.1109/EMBC.2015.7319623

Zou, Q.-H., Zhu, C.-Z., Yang, Y., Zuo, X.-N., Long, X.-Y., Cao, Q.-J., Wang, Y.-F., & Zang, Y.-F. (2008). An improved approach to detection of amplitude of low-frequency fluctuation (ALFF) for resting-state fMRI: Fractional ALFF. Journal of Neuroscience Methods, 172(1), 137–141. https://doi.org/10.1016/j.jneumeth.2008.04.012

VITAE

HANNAH WILD

EDUCATION

University of Kentucky, Clinical Psychology Doctoral Program   2021 - Present
Graduate Student
M.S. *Characterizing Resting Cerebral Blood Flow Abnormalities in Obsessive Compulsive Disorder with Arterial Spin Labeling*

Haverford College, Psychology Department   2015 - 2019
B.S. in Psychology
Minor in Neuroscience

AWARDS AND HONORS

2023	**University of Kentucky College of Arts and Sciences Outstanding Teaching Award**
2022-2024	**UK Psychology Research Assistantship**

RESEARCH EXPERIENCE

Fall 2021 – Present	**University of Kentucky,** Lexington, KY
	Doctoral Graduate Student and Study Coordinator
	The Cognitive Neuroscience and Behavior Therapy Lab
	Advisor: Tom Adams, Ph.D.
2019 - Spring 2021	**National Institute of Mental Health (NIMH)**, Bethesda, MD
	Post-baccalaureate Intramural Research Training Award (IRTA) Fellow
	Lab of Brain and Cognition, Section on Neurocircuitry
	Advisors: Leslie Ungerleider, Ph.D., and Shruti Japee, Ph.D.
Fall 2018 - 2019	**Department of Psychology, Haverford College,** Haverford, PA
	Research Assistant
	Behavioral Neuroscience Lab, Senior Thesis.
	Advisor: Laura Been, Ph.D.
	Cognitive Neuroscience Lab
	Advisor: Rebecca Compton, Ph.D.
Fall 2017	*Animal Care Technician*

PUBLICATIONS

Manuscripts
   Peer-Reviewed Publications

1. Adams, T. G., Kelmendi, B., George, J. R., Forte, J., Hubert, T., **Wild, H.,** Rippey, C., & Pittenger, C. (2023). *Neuroscience Learning and Memory*. Frontopolar multifocal transcranial direct current stimulation reduces conditioned fear reactivity during extinction training: A pilot randomized controlled trial.

2. Fenlon, E. E., Pinciotti, C., Jones, A. C., Rippey, C., **Wild, H**., Hubert, T., Tipsword, J. M., Badour, C. L., & Adams, T. G. (2023). Assessment of comorbid obsessive-compulsive disorder and posttraumatic stress disorder. *Assessment, 31*(1), 126-144. https://doi.org/10.1177/10731911231208403

3. Taubert, J., Japee, S., Patterson, A., **Wild, H**., Goyal, S., Yu, D., & Ungerleider, L. G. (2022). A broadly tuned network for affective body language in the macaque brain. *Science Advances, 8*(47), eadd6865.

4. Compton, R. J., Gearinger, D., & **Wild, H**. (2019). The wandering mind oscillates: EEG alpha power is enhanced during moments of mind-wandering. *Cognitive, Affective, & Behavioral Neuroscience*, *19*(5), 1184-1191.

5. Compton, R. J., Gearinger, D., **Wild, H.,** Rette, D., Heaton, E. C., Histon, S., ... & Jaskir, M. (2021). Simultaneous EEG and pupillary evidence for post-error arousal during a speeded performance task. *European Journal of Neuroscience, 53*(2), 543-555.

6. Hedges, V. L., Heaton, E. C., Amaral, C., Benedetto, L. E., Bodie, C. L., D'Antonio, B. I., Portillo, D. R. D., Lee, R. H., Levine, M. T., O'Sullivan, E. C., Pisch, N. P., Taveras, S., **Wild, H. R**., Grieb, Z. A., Ross, A. P., Albers, H. E., & Been, L. E. (2021). Estrogen withdrawal increases postpartum anxiety via oxytocin plasticity in the paraventricular hypothalamus and dorsal raphe nucleus. *Biological Psychiatry, 89*(9), 929–938. https://doi.org/10.1016/j.biopsych.2020.11.016

7. Hedges, V. L., Heaton, E. C., Amaral, C., Benedetto, L. E., Bodie, C. L., D'Antonio, B. I., Portillo, D. R. D., Lee, R. H., Levine, M. T., O'Sullivan, E. C., Pisch, Natalie P, Taveras, S., **Wild, H.,** Ross, A., Albers, E. H., & Been, L. E. (2020). Estrogen withdrawal alters oxytocin signaling in the paraventricular hypothalamus and dorsal raphe nucleus to increase postpartum anxiety. *BioRxiv*.

CONFERENCE PRESENTATIONS

Poster Presentations

- **Wild, H**., Grazioplene, R., Averill, C., Anticevic, A., Abdallah, C., Pittenger, C., & Adams, T.G. Psychiatric medication influences resting spontaneous neuronal activity in obsessive-compulsive disorder. *Anxiety and Depression Annual Conference,* 2023.

- **Wild, H.,** Fenlon, E., & Adams, T. Attentional control predicts skin picking endorsement and severity. *International OCD Foundation Annual Conference,* 2022.

- **Wild, H.,** Goyal, S., Chung, J., & Japee, S. Relationship between Engagement in Wellness Activities and Mental Health during the COVID-19 Pandemic. *NIMH Scientific Training Day,* September 25, 2020.

- Goyal, S., **Wild, H.,** Chung, J., & Japee, S. How Changes in Exercise, Mindfulness, and Hobby Engagement during COVID-19 relate to Demographics and Self-Reported Indicators of Well-being. *NIMH Scientific Training Day,* September 25, 2020.

- Goyal, S., **Wild, H.,** Herald, S., Duchaine, B., Ungerleider, L., & Japee, S. Processing Facial Expressions in Developmental Prosopagnosia. *Vision Sciences Society*. June 19, 2020.

- **Wild, H.,** Goyal, S., Japee, S., Ungerleider, L., & Taubert, J. Cross-Species Characterization of Facial Expression and Head Orientation Processing. *Vision Sciences Society*. June 19, 2020.

- Goyal, S., **Wild, H.,** Herald, S., Duchaine, B., Ungerleider, L., & Japee, S. Processing Facial Expressions in Developmental Prosopagnosia. *NIH Post-baccalaureate Poster Day*. Bethesda, MD. April 30, 2020.

- **Wild, H.,** Goyal, S., Japee, S., Ungerleider, L., & Taubert, J. Cross-Species Characterization of Facial Expression and Head Orientation Processing. *NIH Post-baccalaureate Poster Day*. Bethesda, MD. April 30, 2020. **(Received an "Outstanding Poster" Award).**

- Gibbons, A.B., Harris, K.C., Singh, A.K., **Wild, H.R.,** Ross, A.P, Albers, H.E., and Been, L.E. Estrogen Withdrawal Increases Anxiety-Like Behavior and Dorsal Raphe Oxytocin Receptors in Female Hamsters. *Society for Neuroscience: Faculty for Undergraduate Neuroscience Poster Session,* San Diego, CA. November 4, 2018.

- Gearinger, D., **Wild, H.,** Thiel, P., and Compton, R. Pupillary and Neural Reactions to Performance Error. *Society for Neuroscience: Faculty for Undergraduate Neuroscience Poster Session,* San Diego, CA. November 4, 2018

SKILLS AND CERTIFICATIONS

Programming
AFNI Proc.py, FSL, MATLAB, R, HTML, Java, CSS, Unix, Python, and CMD

Software
AFNI, FSL, SUMA, SPSS, FileMaker Pro, Scan, Curry, E-Prime, Qualtrics, Tobii Eye Tracker, FaceGen Modeller, Testable, Microsoft Suite, Adobe Photoshop, Final Cut Pro, and Adobe Premiere, Mac, and Windows

Hardware
GE 3T MRI, EyeLink 1000 Plus, Electroencephalography, qPCR, Molecular Biology tasks, Stereotaxic surgery in a hamster model

Neuropsychological Assessments
- Clinician-Administered PTSD Scale for *DSM-5* Training Curriculum
- Diagnostic Interview for Anxiety, Mood, and OCD and Related Neuropsychiatric Disorders (DIAMOND)
- Structured Clinical Interview for DSM-5 Personality Disorders (SCID-5 PD)
- The Zanarini Rating Scale for Borderline Personality Disorder (ZAN-BPD CR)
- The Mini-International Neuropsychiatric Interview (MINI)
- The Wechsler Adult Intelligence Scale-IV, Standard Battery (WAIS-IV)
- The Woodcock-Johnson Test of Achievement-IV, Standard Battery (WJ-IV)